Chemical Engineering & Processing: Process Intensification 117 (2017) 120–140

Contents lists available at ScienceDirect

Chemical Engineering & Processing: Process Intensification

journal homepage: www.elsevier.com/locate/cep

The panorama of plasma-assisted non-oxidative methane reforming

Marco Scapinello, Evangelos Delikonstantis, Georgios D. Stefanidis*

Process Engineering for Sustainable Systems (ProcESS), Department of Chemical Engineering KU Leuven, Celestijnenlaan 200F, 3001 Leuven, Belgium

ARTICLE INFO

Keywords:
Methane coupling
Methane reforming
Ethylene
Plasma-assisted processing
Plasma techniques
Energy efficiency

ABSTRACT

Methane is an important raw material for fuel and commodity chemicals production. Energy-intensive steam methane catalytic reforming in gas-fired furnaces is the main industrial process for methane conversion to synthesis gas and further to other chemicals. Methane conversion by means of non-thermal plasma technologies has attracted attention in the last years, as no pre-heating of the feed-stream at high temperatures is needed. Electric energy is consumed in producing energetic electrons for molecule bonds breaking, instead of gas heating, thereby overcoming the disadvantages of high operational temperatures. In this work, after introducing plasma classification and plasma chemistry, a comprehensive review of literature papers on non-thermal plasma-assisted methane coupling in the period 2010–2016 is presented and the best results that have been obtained with all different kinds of non-thermal plasma techniques are reported. Finally, as the energy cost is the main cost driver of the process after the raw material cost, comparison among all plasma techniques used for methane coupling is performed in terms of specific energy requirement to crack a mole of methane (SER, kJ/mol$_{CH4}$), efficiency (η %) and energy requirement to produce a mole of target product (ER, either kJ/mol$_{C2H2}$ or kJ/mol$_{C2H4}$). This is followed by a comparison between plasma-driven and thermal energy-driven methane coupling.

1. Introduction

Light olefins (i.e. acetylene, ethylene, propylene and butylene) are important building blocks for the production of chemicals, plastics, synthetic fuels and fibres [1,2]. Light olefins are produced through a well-established industrial process, the steam reforming of crude-oil derivatives. However, the crude-oil depletion as well as the significant amounts of CO_2 and NO_x produced in cracking furnaces fuelled the search for alternative feedstocks. Concurrently, recent explorations have discovered an abundance of conventional and unconventional gas reserves rich in methane (i.e. tight gas and shale gas, methane hydrate, coalbed methane) mostly located at decentralised areas, far away from the market [3–9]. The capital intensive gas transportation infrastructure and the energy intensive gas liquefaction process are the main reasons why those gas reserves have not been utilised yet [10–12]. Moreover, the gas released during crude oil extraction at remote reserves is directly flared. In 2012, the total flared gas has been estimated at 143 billion cubic meter, representing ~3.5% of the global natural gas production [13]. Consequently, a potential raw material is depleted and CO_2 is emitted [14,15]. Therefore, there is need to develop technologies for methane gas streams valorisation to added-value products [16].

Various methane reforming technologies resulting in different product distributions have been studied: non-oxidative methane coupling, pyrolysis, partial oxidation and dry and steam reforming are of great interest because the formed products have high commercial value. In non-oxidative methane coupling two methane molecules are directly coupled to acetylene and ethylene at high temperatures (> 1000 °C [17]). Acetylene is widely used in metal constructions (i.e. as oxyacetylene flames or acetylene-air flames for welding) and in chemical industry as precursor for the production of chemicals (i.e. acrylic acid or vinyl monomers), while ethylene is mainly used in the polymer industry and as precursor for other commercial chemicals (acetaldehyde, ethylene oxide and others).

$$CH_4 \rightarrow {}^1/_2\, C_2H_2 + {}^3/_2\, H_2, \quad \Delta H = 193.5\ \text{kJ/mol}\ \text{[non-oxidative coupling to acetylene]} \tag{1}$$

$$CH_4 \rightarrow {}^1/_2\, C_2H_4 + H_2, \quad \Delta H = 101\ \text{kJ/mol}\ \text{[non-oxidative coupling to ethylene]} \tag{2}$$

Methane pyrolysis is used for carbon-free hydrogen and carbon production [18,19].

$$CH_4 \rightarrow C + 2\, H_2, \quad \Delta H = 74.8\ \text{kJ/mol}\ \text{[pyrolysis]} \tag{3}$$

Finally, methane can be reformed by oxygen, carbon dioxide or steam to synthesis gas in different compositions according to the global

* Corresponding author.
E-mail address: Georgios.Stefanidis@cit.kuleuven.be (G.D. Stefanidis).

http://dx.doi.org/10.1016/j.cep.2017.03.024
Received 20 December 2016; Received in revised form 11 February 2017; Accepted 31 March 2017
Available online 12 April 2017

chemistries below [20].

$CH_4 + {}^1/_2\ O_2 \rightarrow CO + 2\ H_2, \quad \Delta H = -35.6$ kJ/mol [partial oxidation] (4)

$CH_4 + CO_2 \rightarrow 2\ CO + 2\ H_2, \quad \Delta H = 247.3$ kJ/mol [dry reforming] (5)

$CH_4 + H_2O \rightarrow CO + 3\ H_2, \quad \Delta H = 206.3$ kJ/mol [steam reforming] (6)

Synthesis gas (syngas) is further used for synthetic fuels production through the Fischer-Tropsch process [21]. In some other cases, the partial oxidation is integrated with dry [22–24] or steam reforming [25,26] enabling the so-called auto-thermal reforming [27–29] (chemistries shown below). Partial oxidation can also be integrated with both dry and steam reforming, making the so called tri-reforming [20,30–33]. The heat released from the exothermic oxidation reaction is absorbed by the endothermic dry and steam reforming reactions. There is not a fixed volumetric ratio of the reactants; methane, oxygen and steam ratios may vary affecting the syngas composition [34,35], which is important for the downstream process.

$CH_4 + {}^1/_2\ O_2 + {}^1/_2\ CO_2 \rightarrow {}^3/_2\ CO + {}^3/_2\ H_2 + {}^1/_2\ H_2O, \quad \Delta H = -15.1$ kJ/mol [autothermal reforming using CO_2] (7)

$CH_4 + {}^1/_4\ O_2 + {}^1/_2\ H_2O \rightarrow {}^5/_2\ H_2 + CO, \quad \Delta H = 85.3$ kJ/mol [autothermal reforming using steam] (8)

As methane is a very stable molecule, owing to the high C—H bond strength (434 kJ/mol [36]), high energy input and high temperatures are necessitated to activate it [37]. Catalysts are usually used to enhance the formation of the desirable product [1,38–42]. The high energy demand and the catalyst instability due to carbon deposition are major drawbacks of the thermal processes. In addition, the short comings of pyrolytic furnaces, such as long start-up/shut-down periods, high volumetric footprint, high capital expenditure and maintenance cost, low energy efficiency in the radiation box, NO_x and CO_2 emissions are considered to be significant process limitations [43,44].

Plasma-assisted methane reforming is currently considered a promising alternative solution [45–47] overcoming most of the issues that thermal processes face. High energy electrons inside the plasma zone generate a huge number of chemically active species, such as radicals, excited species and ions through electron-molecule collisions. The active species can rapidly undergo several chemical reactions [45] under atmospheric pressure and mild temperature ($< < 1000$ °C). Furthermore, relatively low reaction volumes are needed due to the fast reactions and high energy density. Finally, CO_2 emissions diminish if the electricity input is drawn from renewable energy sources. On the downside, plasma is not selective and usually generates wide product distributions.

The high potential of plasma-assisted methane reforming is reflected by numerous research studies, which have been published over the past years. From all possible methane reforming valorisation routes, the current review paper focuses only on non-oxidative plasma-assisted methane coupling and consists of three parts. The first part introduces the concept of plasma and provides basic information about plasma characterization and plasma chemistry. The second part presents the literature studies of the last five years on methane coupling at atmospheric pressure using all possible plasma techniques (dielectric barrier discharge, gliding arc, corona, spark and microwave) and reports the best results that have been achieved with each plasma technique. Finally, the third part makes a comparison among all plasma techniques used for methane coupling in terms of specific energy requirement to crack a mole of methane (SER, kJ/mol_{CH4}), efficiency (η %) and energy requirement to produce a mole of target product (ER, either kJ/mol_{C2H2} or kJ/mol_{C2H4}). This is followed by a comparison between plasma-driven and thermal energy-driven methane coupling.

2. Plasma classification

In thermal plasmas, all generated species have the same temperature since they are in thermal equilibrium. The local thermal equilibrium (LTE) is reached when the mean electron temperature ($T_{electron}$) is equal to the neutral species temperature ($T_{neutral}$). The absolute temperature value is very high, too (approximately in the order of 10^4 K). Under such conditions, the active species are indistinctly produced by thermal activation or electron collisions. Arc discharges form characteristic example of thermal plasmas and they are widely used in specific applications, where high temperature is required (i.e. metallurgy, acetylene synthesis).

In non-thermal plasmas, the temperature of the different plasma species varies substantially. The energy is preferentially channelled to the electrons, which subsequently transfer it to the heavier species through electron-molecule collisions. The temperature sequence of the plasma species in non-thermal plasmas is: $T_{electron} > > T_{ions} > T_{neutral}$. Dielectric Barrier Discharges (DBD), corona (DC, AC and pulsed) and nanosecond pulsed discharges are usual examples of non-thermal or cold plasmas.

It has been observed, however, that some arcs do not reach the LTE even though the temperature is rather high. Moreover, in some non-thermal plasmas the neutral species have relatively high temperature ($T_{neutral}$ about 10^3 K). In the aforementioned cases, the discharges show intermediate behaviour. Non-thermal plasma models cannot describe accurately the phenomena that take place in those discharges; therefore, thermal activation cannot be neglected. Only recently, those discharges have been grouped in a third category known as “warm plasmas” [48]. Microwave, radio frequency, glow and spark discharges belong to this group.

3. Plasma chemistry: reaction mechanism

A simple rationalization of methane dissociation mechanism in a plasma discharge is not possible. Differences in plasma characteristics due to different plasma techniques and discharge conditions do not permit a unique treatise; therefore, different models have been developed. Some models take into account only reaction kinetics while other models are more advanced including also fluid dynamics. Some authors have developed unique models to describe specific plasma techniques such as Thermal Arc [17], DBD [49,50], MW [51], Gliding Arc [52] or DC micro-glow [53] while others have taken into account general conditions and extended the results to describe different discharges [36,54,55].

3.1. Plasma chemistry for thermal plasma

Thermal plasmas have been extensively studied and also applied at industrial scale (i.e. Hüels [56] process for acetylene synthesis). Fincke et al. [57] and Fridman [58] have reported on the thermodynamics, kinetics and other aspects of the process. In arc discharge, the mixture of neutral and ionic species is at thermal equilibrium. Kovács et al. [59] have demonstrated that at a temperature higher that 4000 K the reactivity of ionic species is considerably lower than that of neutral species. Therefore, the decomposition of methane is driven by thermal activation because high temperature provides sufficient energy for the activation of the dehydrogenation reaction. The reaction generally follows the Kassel mechanism: primary ethane is produced through methane dehydrogenation to methyl radicals (CH_3) and subsequent CH_3 recombination; then, a cascade of dehydrogenation reactions to ethylene (10^{-6}–10^{-5} s), acetylene (10^{-4}–10^{-3} s) and eventually to carbon and soot take place according to the reaction scheme below.

$CH_4 \rightarrow C_2H_6 + H_2, \quad \Delta H = 0.7$ eV/mol (9)

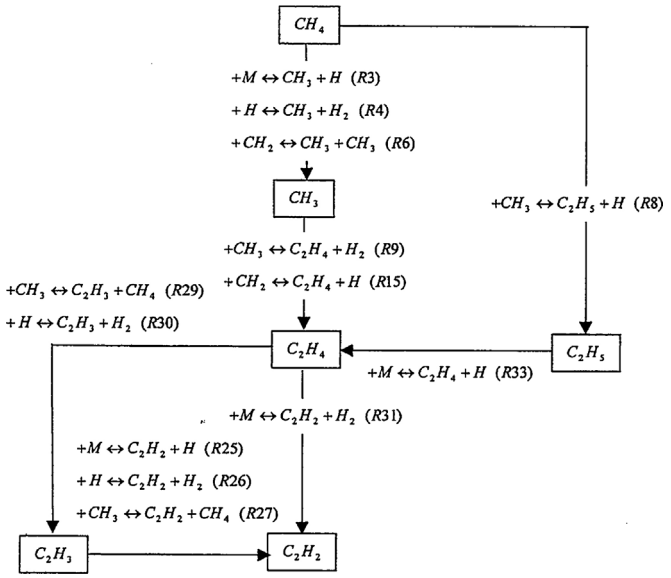

Fig. 1. Predominant reaction mechanism for formation of acetylene. Reproduced with permission from Fincke et al. (2002).

$$C_2H_6 \rightarrow C_2H_4 + H_2, \quad \Delta H = 1.4\ \text{eV/mol} \tag{10}$$

$$C_2H_4 \rightarrow C_2H_2 + H_2, \quad \Delta H = 1.8\ \text{eV/mol} \tag{11}$$

$$C_2H_2 \rightarrow 2\,C_{(s)} + H_2, \quad \Delta H = -2.34\ \text{eV/mol} \tag{12}$$

More elaborate reaction mechanisms introduced by other authors take into account the different intermediate reactions; such an example is shown in Fig. 1. However, the last stage, being the conversion of acetylene to soot is not fully understood yet even though detailed models have been developed to describe soot formation. For example, Slovetskii et al. [60] considered the growth of soot particles as a polymerization reaction of acetylene in an arc plasma torch, while Fincke et al. [57] introduced the benzene production mechanism, where benzene serves as a precursor of polycyclic aromatic hydrocarbons (PAH).

3.2. Plasma chemistry for non-thermal plasma

For non-thermal plasmas, it is universally agreed that the gas phase is far from equilibrium and the complexity of the system requires a step evolution: the formation of radicals by electron impact reactions and, once radicals are generated, propagation and recombination reactions in order to obtain the final products. This is generally agreed for DC micro-discharges [53] and macro-discharges [54] representing MW and capacitive discharges. Moreover, in nanosecond pulsed discharges and DBD micro-discharges, it is possible to separate the first stage (during the pulse) from the second one (afterglow). Consequently, two different kinetics schemes are usually adopted to describe the whole process: one is valid when the discharge is on and the other one when it is off during the so called afterglow period [54,61].

To understand the electron impact reactions, it is necessary to analyse the generation of non-thermal plasma. The presence of a strong electric and/or magnetic field forces the free electrons to accelerate. The electrons increase their velocity and, consequently, their kinetic energy ($E_{kin} = 3/2\ k_B T$). Generally, in atmospheric pressure plasma, $T_{electron}$ ranges between 1 and 5 eV. Because of the in homogeneity of the electric field, it is useful to describe the electron energy introducing the electron energy distribution function (EEDF) f (ε), which is the probability density for an electron to obtain an energy value ε. Electron energy follows the Maxwell Boltzmann distribution. Electrons collide with other plasma components, transmitting part of their energy and providing energy for ionization, excitation, dissociation and other plasma chemical reactions. The rates of these elementary reactions depend on the number of effective collisions and thus on the density of the electrons with a specific energy. Low electron energy may result in vibrational excitation, medium electron energy in molecular dissociation and high electron energy in molecular (dissociative) ionization. In the case of non-oxidative methane coupling, the most important electron-impact reactions are listed below [45]:

Vibrational excitation

$$CH_4 + e^- \rightarrow CH_4\ (v24) + e^-, \quad \text{Threshold energy} = 0.162\ \text{eV} \tag{13}$$

$$CH_4 + e^- \rightarrow CH_4\ (v13) + e^-, \quad \text{Threshold energy} = 0.361\ \text{eV} \tag{14}$$

Dissociation

$$CH_4 + e^- \rightarrow CH_3 + H + e^-, \quad \text{Threshold energy} = 9\ \text{eV} \tag{15}$$

$$CH_4 + e^- \rightarrow CH_2 + H_2 + e^-, \quad \text{Threshold energy} = 10\ \text{eV} \tag{16}$$

$$CH_4 + e^- \rightarrow CH + H_2 + H + e^-, \quad \text{Threshold energy} = 11\ \text{eV} \tag{17}$$

$$CH_4 + e^- \rightarrow C + 2\,H_2 + e^-, \quad \text{Threshold energy} = 14\ \text{eV} \tag{18}$$

Ionization [62]

$$CH_4 + e^- \rightarrow CH_4^+ + 2\,e^-, \quad \text{Threshold energy} = 12.75\ \text{eV} \tag{19}$$

$$CH_4 + e^- \rightarrow CH_3^+ + H + 2\,e^-, \quad \text{Threshold energy} = 14.3\ \text{eV} \tag{20}$$

$$CH_4 + e^- \rightarrow CH_2^+ + H_2 + 2\,e^-, \quad \text{Threshold energy} = 15.1\ \text{eV} \tag{21}$$

$$CH_4 + e^- \rightarrow CH^+ + H_2 + H + 2\,e^-, \quad \text{Threshold energy} = 22.2\ \text{eV} \tag{22}$$

$$CH_4 + e^- \rightarrow C^+ + 2\,H_2 + 2\,e^-, \quad \text{Threshold energy} = 25\ \text{eV} \tag{23}$$

Due to the high electron energy required for ionization reactions, only few electrons may result in gas ionization. Therefore, the ionization degree of non-thermal plasmas gases ranges between 10^{-4}–10^{-7} [58]. Although a scarce number of electrons lead to ionization, ionization reactions are important because they sustain the discharge.

Primary radical species are formed through dissociation electron impact reactions. The rate of CH_i (i = 0–3) radical production and the fragmentation pattern depend on the methane collision cross section and the electron energy distribution function (EEDF) at given conditions. Nozaki et al. [63] studied the fragmentation pattern in a DBD as function of the reduced electric field strength (E/N, Td), defined as the electric field strength (E, V/cm) divided by molecules density (N, cm^{-3}). Specifically, they observed that at low E/N (< 500 Td), the electrons initiated the methane dehydrogenation reaction and CH_3 was the prevailing radical (60% selectivity at 80 Td; 1 Td = 10^{-17} V cm^2). At higher E/N values, the prevailing radicals were CH_2, CH and C. Consequently, the final product distribution differed.

Yang [55] developed a model to describe the final product formation (Fig. 2). In this context, they defined the energetic threshold of ethane to acetylene formation transition: ethane was predominant at low energy input (< 70 eV/molecule), low concentration of electrons and energy > 6 eV (typical for DBD), while at higher energy input (> 100 eV/molecule), high concentration of electrons and electron energy > 13 eV, acetylene became the dominant product. The same observation has been made for corona discharges, where the primary streamer head possesses an average energy in the range of 10–20 eV. Kado et al. [64] studied these fragmentations at high input energy using a pulsed spark discharge and isotopic gases.

It is interesting to mention that during inelastic collisions, only a

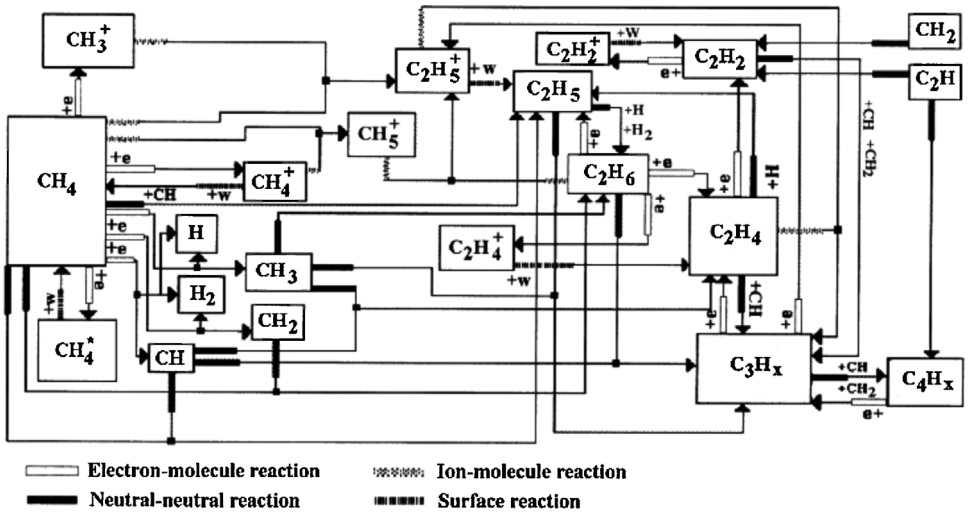

Fig. 2. Schematic showing the dominant reaction paths for C2 and C3 hydrocarbon products in the plasma under typical conditions: atmospheric pressure, pure methane feed. Reproduced with permission from Yang (2003).

part of the electron energy is channelled to dissociation and ionization reactions, while a considerable part is transferred to vibrational excitation reactions. Yang et al. [55] and De Bie et al. [50] considered the excitation reactions in their models and balanced them with the de-excitation process occurring on the reactor wall. Contrariwise, Ravasio and Cavallotti [54] did not consider any excited species in their model, which likely leads to underestimation of the plasma reactivity as well as overestimation of the energy efficiency. Nozaki et al. [36] showed that the vibrational excitation channel was the most prevalent and the density of vibrational excited methane species was 150 times higher than the electron density. In their model, the vibrational excitation reactions are considered as the only energy sink in the set of electron-molecule collisions; specifically, ~36% of the electrical energy input was consumed and lost in this channel. However, the vibrational excited methane species are supposed to enhance the catalytic methane conversion. Therefore, they are considered as key species in hybrid single-stage plasma–catalytic systems.

After the primary radical generation, the reaction mechanism is dominated by radical recombination reactions. Radical-radical, radical-neutral and neutral–neutral reactions (and also ionic chemistry if taken into account) are strongly dependent on the gas temperature. Regarding the electron impact reactions, it is not clear yet whether they are totally gas temperature independent. The gas temperature is critical because it determines which reactions will be activated. The gas temperature impact can be plainly explained with the following examples of acetylene formation and methyl radical creation: in a DBD, the acetylene is formed by ethylene dehydrogenation and other hydrocarbon species radical reactions [50], whereas in pulsed corona discharge (PCD) as well as other discharges with higher energy electrons than the DBD, acetylene formation is dominated by hydrogenation of C_2 radicals and CH dimerization [65]. Methyl radicals (CH_3) are mainly generated through electron dissociation reactions as primary radicals. However, if the temperature is higher than 1000 K, a secondary channel is thermally activated and methane dehydrogenation is promoted by H radicals (e.g. $CH_4 + H \rightarrow CH_3 + H_2$). That thermally activated channel is prevailing in all warm discharges [54] and is an important route for H_2 production and methane reforming in MW plasma [51] and Gliding Arc [52].

For the aforementioned reasons, the thermal activation must be taken into account in warm discharges. First Indarto et al. [52] and later Dors et al. [51] developed simplified kinetic models for Gliding Arc and MW, respectively, taking into account the thermal effect. Specifically, Dors and his co-workers developed a model tailored to methane combustion. Electron impact reactions were not considered due to the low reduced electric field E/N (about 1 Td), so the amount of energy was not enough to activate direct dissociation and ionization reactions. In this model, the chemical kinetics were solely controlled by the thermal effect while electron impact reactions had no contribution. Their experimental results were aligned with the theoretical ones given by the thermal equilibrium in the temperature range 1500–2000 K, where radical-involved reactions are activated such as methane, ethane and ethylene dehydrogenation promoted by H radicals in addition to classical Kassel mechanism reactions.

$$H + CH_4 \rightarrow CH_3 + H_2 \quad (24)$$

$$H + C_2H_6 \rightarrow C_2H_5 + H_2 \quad (25)$$

$$C_2H_5 \rightarrow C_2H_4 + H \quad (26)$$

$$H + C_2H_4 \rightarrow C_2H_3 + H_2 \quad (27)$$

$$C_2H_3 \rightarrow C_2H_2 + H \quad (28)$$

These dehydrogenation reactions are activated at high temperature, in the range 1000–1300 K as Ravasio and Cavallotti [54] indicated in their model for macro-discharges, which can also be applied to describe MW plasma. The temperature (1500–2000 K) indicated by Dors et al. [51] for the same reactions is very far from the temperature of the plasma region (4000–5700 K). Their explanation about this temperature difference is that methane reforming reactions take place in the swirl gas flowing around the plasma and not in the plasma zone itself.

4. Plasma-assisted methane coupling

Plasma-assisted methane conversion to added-value products is a popular research subject in the plasma community. Different input parameters have been studied in order to achieve high CH_4 conversion and olefins yield per reactor pass; the most important parameters are the applied voltage, feed flow rate and pulse repetition frequency.

Applied voltage strongly modifies the strength of the electric field and consequently the plasma characteristics ($T_{electron}$, electron density and so discharge current). For a given reactor configuration and constant flow rate, applied voltage drives the discharge power. Generally, higher discharge power leads to higher CH_4 conversion due to the increased frequency of electron-molecule collisions. The CH_4 dissociation rate is also higher and C_2hydrocarbons are the dominant products. Product selectivity depends on the synergistic effect of different input parameters; therefore, it is difficult to draw a general

conclusion. However, it has been verified that high energy input promotes carbon formation. Energy input is the dominant and most well studied parameter.

For a given reactor configuration and specific applied voltage, the feed flow rate directly influences CH_4 conversion because both the residence time and specific energy input (SEI) change. Feed flow rate increase causes residence time and SEI decrease. Shorter residence time and lower SEI result in decreased probability of collision of CH_4 molecules with highly energetic electrons and active species. As a result, conversion decreases.

Frequency is also connected with the energy input ($E = E_{pulse}$ f). At low values, frequency does not considerably affect CH_4 conversion and product selectivity. However, for values higher than 10 kHz, frequency starts to play an important role in discharge performance. Physics and chemistry change due to the presence of ionic remnant and memory effect become important. Some authors have reported that the presence of ionic remnant decreases the energy needed for discharge initiation and, as a consequence, higher conversion is achieved.

Sophisticated electrode configurations (geometry) have also been constructed and proposed as an effective way to affect the discharge characteristics and enhance the product yield. It has been observed that sharp edges enhance locally the electric field while short discharge gaps increase the electron density, resulting, in both cases, in higher CH_4 conversion.

Co-feeding of CH_4 with noble or reactive gases has also been applied to increase either CH_4 conversion or certain product selectivity. Particularly, reactants, such as N_2, O_2, H_2O (steam) and other hydrocarbons, have been used together with CH_4 for different reasons, being the study of different reactions, the reproduction of realistic feed compositions, or to suppress of carbon formation. In other cases, noble gases (mainly Ar) have been used as carrier gases. Noble gases do not undergo chemical transformation; they only modify the CH_4 activation mechanism during the course of the plasma reaction. It has been specifically shown that metastable Ar* species, which are formed inside the discharge act as energy carriers for the reaction. Energy is transferred from excited atoms and excited molecules (Ar*) to ground state atoms and molecules. This is called the Penning ionization phenomenon [66].

Finally, integration of plasma and catalytic CH_4 coupling in common chamber of hybrid reactors reflects the high interest of plasma researchers to optimise and intensify this process. The synergistic effect of hybrid plasma-catalytic reaction systems has been thoroughly investigated in the last six years. Specifically, the impact of the catalyst chemical, physical and electrical properties, such as composition, surface, shape, size and electric conductivity, on the plasma characteristics and, as a consequence, on CH_4 conversion and product selectivity have been studied. It has been noticed that vibrationally excited species, which are formed inside the plasma zone and considered to be the main energy sink in plasma systems (Nozaki et al. [36]), enhance the catalytic reaction performance due to the higher internal energy of molecules, while the presence of catalyst increases the local electric field strength. Moreover, discharges occur on the catalyst surface, instead of the confined filaments when no catalyst is used, thus enhancing CH_4 conversion further. However, carbon formation in gas phase always takes place in these conditions and represents an open problem for the adoption of a catalyst into the plasma zone. Indeed, carbon is deposited on all surfaces, including reactor walls and catalyst particles, thereby decreasing the active surface of the catalysts and poisoning the catalytic action [67]. After a certain period of operation, catalyst stability is compromised and regeneration is needed. In addition, specifically in plasma-catalyst systems, short circuits created by conductive carbon interrupt the discharge initiation.

All the published results since 2010 regarding the study of the aforementioned parameters and their impact on the plasma-assisted CH_4 coupling are grouped and reported for each plasma technique in the ensuing sections. At the end of each section, a brief analysis of performance of each plasma technique in terms of conversion and product selectivity (ethane in the case of DBD and acetylene for the other discharges) as function of the Specific Energy Input (SEI) is presented. For sake of clarity, SEI is calculated as the power supplied into the discharge over the feed flow rate [$kJ\,l^{-1}$]. All the presented data are taken from the literature.

4.1. Dielectric barrier discharge (DBD)

DBD (or silent discharge) is the electrical discharge that occurs between two electrodes (planar or cylindrical) separated by an insulating material (dielectric barrier). Alternating voltage (AC) is required for the operation of this type of discharge. DBD is used in CH_4 conversion to valuable products at atmospheric pressure; the highly energetic electrons generated in the plasma zone offer a convenient way to process gases and produce added-value chemicals. Scalability and ease of sustaining the non-thermal plasma are the main advantages of this type of plasma reactor [68]. Low CH_4 conversion, poor product selectivity and high energy cost are important drawbacks. Recently, DBD microplasma reactors have been used for gases conversion to tackle the limitations of conventional DBD reactors; their smaller space may imply a stronger electric field and higher concentration of electrons and radicals. They also combine the advantages of non-thermal plasma with those of microreactors, offering better control of processing parameters for the selective synthesis of particular products. The results for CH_4 coupling in both conventional and micro DBD reactors are reported below.

When varying the intensity of the input parameters such as applied voltage, feed flow rate, frequency and pulse duration (in case of pulsed discharge), the plasma characteristics change. This is well-known to plasma scientists; therefore, a lot of work has been done on parametric studies. Lü and Li [69] attempted to develop a process to convert CH_4 to C_2 hydrocarbons using non-thermal plasma in a DBD reactor at room temperature and atmospheric pressure. They noticed that CH_4 conversion increased and C_2 hydrocarbon selectivity decreased when the applied voltage increased. In other series of experiments, they noticed that CH_4 conversion decreased and C_2 selectivity increased when the inlet feed flow rate increased. In the range of 20–40 mL/min, the maximum CH_4 conversion and C_2 selectivity achieved were 47% and 40%, respectively. Wang et al. [70] investigated direct conversion of pure CH_4 to higher hydrocarbons in both a co-axial micro-DBD reactor (the plasma is confined in a gap < 1 mm) and a conventional DBD reactor (gap = 1.9 mm) at atmospheric pressure. The effects of input power, residence time (via changing the feed flow rate for a given reactor volume), discharge gap and external electrode length on CH_4 conversion and product selectivity were studied. Micro-DBD performed better than conventional DBD. The highest CH_4 conversion and $C_2 + C_3$ selectivity reached 25.1% and 80.27%, respectively, in the micro-DBD reactor with the following characteristics: gap = 0.4 mm, external electrode length = 100 mm, input power = 25 W, residence time = 4.11 s and feed flow rate = 20.24 mL/min.

Xu and Tu [71] developed a cylindrical DBD reactor of 90 mm length, 3 mm gap, maximum Voltage of 40 kV and volume = 13.6 cm^3 specifically for H_2 production and other added-value products from pure CH_4. They explored the impact of input power, residence time and pulse repetition frequency on CH_4 conversion. The highest CH_4 conversion was 25.2% at a feed flow rate of 50 mL/min, discharge power 45 W and frequency 20 kHz. They found out that the residence time of CH_4 inside the discharge zone had the most significant effect on both CH_4 conversion and H_2 yield; specifically, by increasing the residence time, CH_4 conversion increased almost linearly, while C_2 hydrocarbons selectivity significantly decreased and $C_3 + C_4$ selectivity

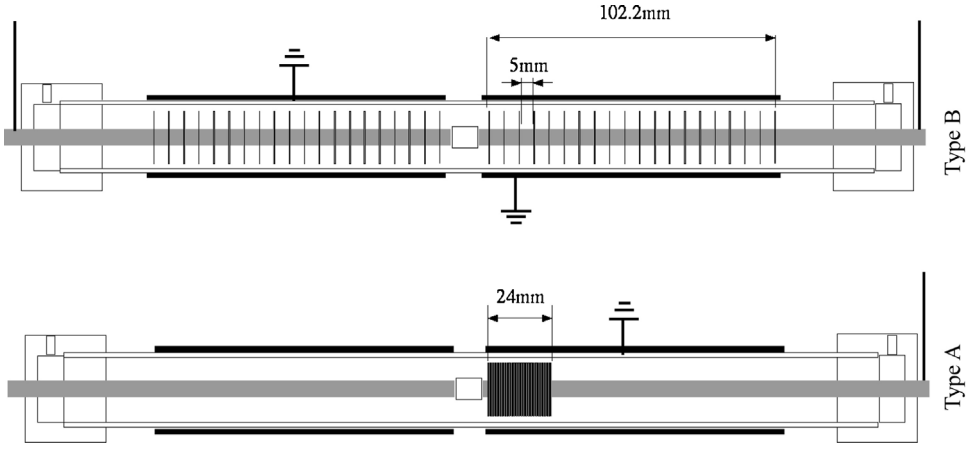

Fig. 3. Electrode configurations, which Kono et al. used in their experiments. (a) Type A reactor: 40 discharge disks set at 0 mm interval and placed in a dense area on the co-axial 24 mm long wire; (b) 40 sheets placed on the co-axial rod with 5 mm intervals.
Reproduced with permission from Kono et al. (2015).

slightly increased. Conversion of CH_4 slightly decreased by changing the pulse repetition frequency (weak effect).

Liu et al. [72] also investigated the conversion of CH_4 to H_2 and higher hydrocarbons in a co-axial DBD reactor at atmospheric pressure and low temperature. They also confirmed that input power was the most essential parameter while the excitation frequency was the least important one. In particular, conversion of CH_4 increased almost linearly with increase in input power (from 15 W to 75 W) and reached a maximum value of 36%. Higher input powers strengthened the electric field resulting in higher electron density and energy. Higher number of electrons with high energy (sufficient for methane reforming) increased the conversion. Consequently, selectivity to H_2 was increased by a factor of 2 while H_2 yield increased 4 times when the input power increased from 15 W to 75 W. Concurrently, C_2H_2 and C_2H_4 selectivity decreased but the selectivity of saturated hydrocarbons (C_2H_6, C_3H_8 and C_4H_{10}) increased. As far as the effect of flow rate is concerned, the authors showed that CH_4 conversion and H_2 yield decreased when the feed flow rate increased, while selectivity to C_2 hydrocarbons significantly increased. Selectivity of C_3 and C_4 decreased 3 times with increase infeed flowrate. Nishida et al. [73] studied the effect of the high voltage pulse width on CH_4 and C_3H_8 conversion to obtain higher decomposition rates. Pulses with width higher than 10 μs were composed by multiple pulses of 5 μs (e.g. 20 μs = 4 × 5 μs). They concluded that multiple short pulses resulted in more efficient decomposition because each short pulse generated a separate discharge in which a plasma decomposition reaction occurred. Multiple pulses corresponded to more plasma discharges, resulting in high decomposition rate. They also suggested the use of multiple narrow pulses as a high voltage source. In such short discharges, the physical phenomena depend on the life time of plasma produced by each pulse.

Plasma reactor design is essential for the reactor performance. Different parts of a reactor, such as electrodes and dielectric barriers as well as the discharge gap can affect the electric field strength. Consequently, the characteristics of plasma change too. Konno et al. [74] investigated the effect of inner HV electrode configuration on CH_4 conversion and selectivity to light hydrocarbons (C_2H_6, C_3H_8, etc.) in a DBD plasma reactor at atmospheric pressure. They built and tested two different electrode configurations (Fig. 3): one with 40 discharge disks set at 0 mm interval and placed in a dense area on the co-axial wire of 24 mm (Type A) and one with 40 sheets placed on the co-axial rod with 5 mm intervals (Type B). The authors reported that CH_4 conversion in Type B was always higher than Type A for a given input power. The presence of discharge disks intervals led to higher CH_4 conversion because the discharge occurred in the gap between the discharge disks and the dielectric barrier resulting in higher spike density as compared with the reactor without intervals between the disks.

The electrode material and the dielectric barriers are also considered as factors, which may influence the reactor performance. For instance, Kundu et al. [75] studied the reforming of CH_4 to higher hydrocarbons in a DBD reactor (length 300 mm, maximum voltage 20 kV, frequency 21.5 kHz) in excess of Ar and at atmospheric pressure using alumina (23 mm OD, 2.0 mm wall and 10 mm OD, 1.0 mm wall) and quartz (25 mm OD, 1.8 mm wall and 12 mm OD, 1.5 mm wall for quartz) as dielectric barriers. Due to the different capacitive properties of those materials, the discharge power differed for a given applied voltage; therefore, CH_4 conversion and H_2 yield varied too. Alumina was found to be a more suitable material for CH_4 conversion than quartz (CH_4 conversion 3.6 mmol/h vs 3.1 mmol/h, respectively). This is explained by the physics of discharge and the materials properties namely the fact that the charge transferred in a micro-discharge is proportional to ε/g, ε being the relative permittivity and the thickness of dielectric [68]. Alumina has lower dielectric strength than quartz (16.7 kV/mm vs 25 kV/mm), thus it requires higher thickness and higher relative permittivity (9.8 vs 3.75). The combination of those two parameters contributes to higher capacitance and so, the dissipated power into the reactor increases.

Nishida et al. [76] investigated the synergistic effect of the electrode geometry and the construction material on CH_4 and C_3H_8 reforming at high pressure (over 1.5 atm) in a DBD reactor (pulse duration 5 μs, frequency 2–4 kHz) in order to build an on-board system for H_2 production with high efficiency and high production rate. Initially, they modified the size of the inner electrode to affect the volume of the DBD reactor chamber. A bolt and a multibolt inner electrode configuration were used. In the case of multibolt inner electrode, the charge was localised due to wrinkled surface. Moreover, the total discharge volume was 60% of the volume of the smooth electrode. The authors also used Pyrex glass and ceramics (Al_2O_3) as dielectric materials. However, they observed that only Al_2O_3 could tolerate high power discharges over a long period (several hours). It was concluded that the largest electrode with the multibolt shape achieved the highest CH_4 conversion, but its performance was dependant on temperature. In another work [77], the authors used a pin type inner electrode with 16-pin electrodes over the circumference of the ring and seven pairs were set up in between nuts and washers to fix pin electrodes. That electrode showed the lowest conversion among all types of electrodes used because the discharge was initiated only on the edge of the tip.

Adding a gas inside the plasma discharge may affect the chemistry. It strongly depends on the type of gas. When noble gases are added in gas discharges, the plasma characteristics are modified. The physical (i.e. the breakdown voltage) and chemical properties (i.e. adding

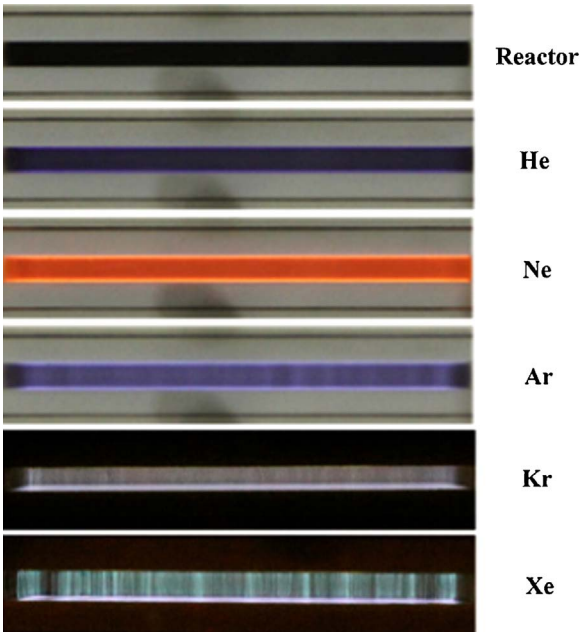

Fig. 4. Discharge images from mixtures of 10 vol% CH_4 and 90 vol% of different noble gases at an applied voltage of 5.0 kV.
Reproduced with permission from Jo et al. (2014)

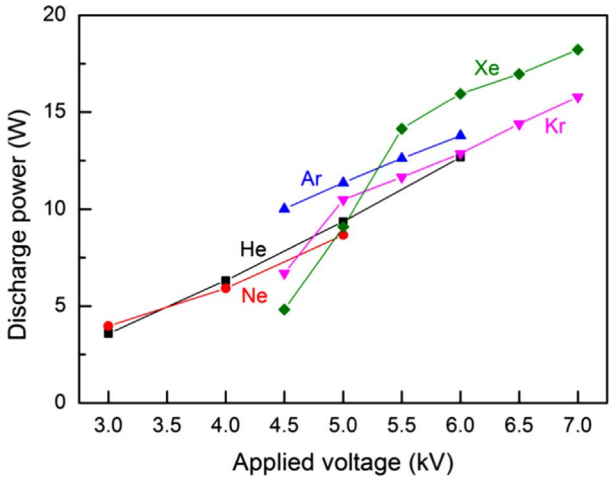

Fig. 5. Measured discharge power versus applied voltage for different noble gases.
Reproduced with permission from Jo et al. (2014)

metastable species) of the discharge change, but the final chemistry is not affected because noble gases are not reactive. They only act as energy carriers transferring their energy to the gas molecules and opening new conversion channels.

Many studies have been conducted on testing the influence of noble gases on electron density, electron temperature and breakdown voltage, and, as a consequence, on CH_4 conversion and product selectivity. Jo et al. [78–80] studied the activation of CH_4 (10%$_{vol}$) in the presence of various noble gases (90%$_{vol}$), such as He, Ne, Ar, Kr and Xe (Fig. 4), in a DBD reactor with the following characteristics: gap 3 mm, volume 4 cm^3, feed flow rate 336 cm^3/min, maximum voltage 10 kV, frequency 50 kHz. They applied identical conditions to evaluate and compare the discharge power for each noble gas addition (Fig. 5). The main products were alkanes (C_2H_6 and C_3H_8) and alkenes (C_2H_4 and C_3H_6), which were produced due to the magnitude of the reduced field ~70 Td irrespectively of the noble gas addition.

Kr was found to be the most suitable noble gas for CH_4 conversion (Fig. 6A). Jo et al. [78–80] noticed that for He and Ne, the discharge power was higher than 12.7 W and 8.7 W, respectively, resulting in arc discharge transition. Excited and ionized species as well as electron temperature and electron density should be considered when comparing CH_4 conversions in the presence of Ar, Kr and Xe because the active species of these noble gases have dominant roles in CH_4 activation. Generally, a noble gas can affect CH_4 conversion by increasing the electron temperature and the density of electrons and active species. The differences in the energies and densities of electrons and active species (Fig. 6B) stem from the intrinsic characteristics of each noble gas (breakdown voltage and energetic thresholds of reactions, which generate excited or ionized species).

A detailed study (effect of CH_4/Ar mole ratio, feed flow rate, input voltage, and reactor configuration) was done by Wang et al. [81] on direct conversion of CH_4 to higher hydrocarbons in a co-axial DBD microreactor at atmospheric pressure. They proved that CH_4 conversion and product selectivity change with CH_4:Ar molar ratio at a fixed feed flow rate. In their experiments, the CH_4:Ar molar ratio varied from 1:3 to 3:1 to verify its effect while the feed flow rate and applied voltage were kept constant. By increasing CH_4 concentration in the feed, the specific energy input (kJ/mol$_{CH4}$) decreased, thus CH_4 conversion rapidly decreased. Consequently, as the energy input was low, dissociation reactions mainly led to CH_3 radical formation rather than to CH_2 and CH. Therefore, selectivity of C_2H_2, C_2H_4 and H_2 decreased while selectivity of C_2H_6 and C_3H_8 increased. By increasing the feed flow rate, CH_4 conversion decreased but the product selectivity did not change. When input power increased, CH_4 conversion increased. The product selectivity slightly changed except for C_2H_6, which decreased. Carbon formation increased too. They also tested two different discharge gaps (0.9 mm and 0.5 mm) and proved that the lowest discharge gap is the most suitable for CH_4 conversion considering the same residence time and the same energy input. Although differences in CH_4 conversion

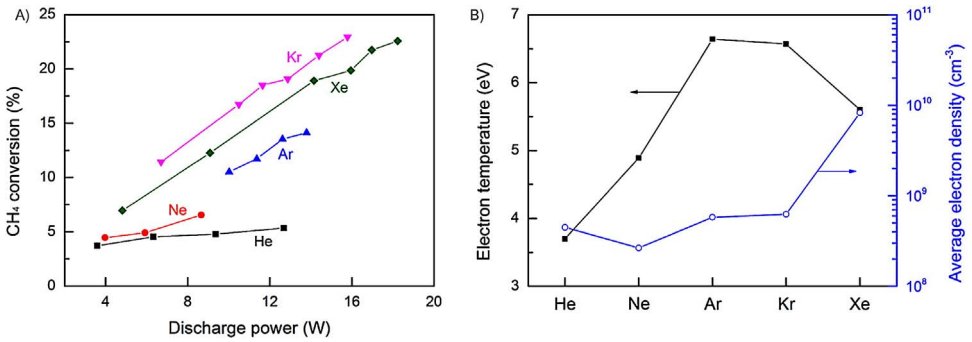

Fig. 6. (A) conversion of methane versus discharge power for all noble gases; (B) calculated average electron temperature and average electron density for all noble gases at the following discharge powers: He: 12.7 W; Ne: 8.7 W; Ar: 13.8 W; Kr: 14.4 W; Xe: 14.1 W.
Reproduced with permission from Jo et al. (2014)

were reported, very similar product selectivity was achieved in both discharge gaps.

Khalifeh et al. [82] focused on the decomposition of CH_4 to H_2 using a nanosecond pulsed plasma DBD reactor in presence of argon. Different active volumes (based on different grounding electrode length), voltages and frequencies were tested to investigate the reactor performance in terms of methane conversion, hydrogen production rate and energy efficiency. The maximum CH_4 conversion and H_2 production rate were 87.2% and 0.3567 mmol/min, respectively. Increase in pulse repetition frequency at different applied voltages enhanced CH_4 conversion and H_2 production up to the frequency of 10 kHz. At higher repetition frequencies, variation of the applied voltage did not significantly affect CH_4 conversion and H_2 production.

Reactive gases have also been added in gas discharges to enhance the desired product formation. For example, Horvath et al. [62] used a mixture of N_2 and CH_4 in various ratios (N_2:CH_4 = 98:2, 95:5, 90:10) at atmospheric pressure and ambient temperature. This mixture simulated Titan's atmosphere and provided some insights into the prevalent chemical processes that take place there. A co-axial packed bed DBD reactor filled with borosilicate glass balls of 6 mm was employed for the experiments. The main chemical products obtained were HCN, C_2H_2 and C_2H_6 with small but significant traces of NH_3 (yields: HCN > C_2H_2 > C_2H_6 > NH_3) and a brown-yellowish deposit on the central rod and the dielectric pellets. They noticed that by increasing the initial CH_4 content, the concentrations of most of the products increased, but the concentration of HCN did not (HCN formation was lower than the other products at higher initial CH_4 concentrations). They also observed that energy input increase resulted in higher HCN and NH_3 formation. The gas flow rate had a significant effect on the residence time; at low flow rates, the residence time increased and significant recombination processes occurred resulting in higher hydrocarbon and nitrile yield. Eventually, Horvath et al. [62] recommended a packed bed DBD as a promising technology for HCN and NH_3 in terms of energy demand. The impact of N_2 addition was explicitly investigated by Snoeckx et al. [61] who co-fed N_2 both as impurity and as carrier gas with CH_4 in a DBD. Kinetic models were also developed to fully understand the influence of N_2 concentration on H_2 production from CH_4. They highlighted the importance of $N_2(A^3\Sigma_u^+)$ and $N_2(a'^1\Sigma_u^-)$ metastable states in CH_4 conversion and H_2 production. When N_2 was used as impurity (1–50000 ppm), CH_4 conversion and H_2 yield decreased due to the electron attachment effect of N_2. When N_2 was used as reactant gas (1, 10, 19, 29, 39, 48, 58, 67, 77 and 87%) to produce nitrogen-containing compounds, it was noticed that for low N_2 content (0 to 17.5% content), CH_4 conversion slightly decreased first, due to the decreasing electron density with increasing N_2 content. Subsequently, it increased up to 70% due to the presence of N_2 metastable species, which enhanced CH_4 conversion. Above 70%, the increasing trend started to become more significant.

4.1.1. Integration of plasma-catalytic reactions

The enhancement of catalytic reactions by plasma motivated many researchers to perform CH_4 coupling in hybrid plasma-catalytic systems and investigate the interactions between plasma and catalytic phenomena. Nishida et al. [77] investigated the impact of the catalyst placement inside the plasma zone and compared the performance of a DBD reactor at 1.5 bar with and without catalyst. The selected catalyst was $BaTiO_3$ in pellets and CH_4 and C_3H_8 were used as feedstock. They did not observe any difference when the catalyst was placed inside the plasma zone. However, after a long operation period, the discharge could not be initiated in the packed reactor because carbon was deposited on the catalyst particles and short circuits were created. In other works, input parameters varied to investigate their impact on such hybrid systems. Rahimpour et al. [46] studied the impact of applied voltage on continuous co-cracking of CH_4 and *n*-$C_{16}H_{34}$ (*n*-hexadecane) over a Mo-Ni/Al_2O_3 catalyst in a cylindrical packed bed DBD plasma reactor with a unipolar-pulsed high voltage source at ambient pressure and temperature. Light hydrocarbons (C_2, C_3, C_4) and H_2 (the main component) were formed. Rahimpour and his co-workers also confirmed that applied voltage is the dominant parameter and they proposed the integrated plasma-catalyst configuration as the most efficient system for reforming, as compared with pre- and post-plasma systems.

Khalifeh and co-workers [83] studied the impact of carrier gas flow (Ar), input discharge power and CH_4 flow rate on energy efficiency and coke formation, using three plasma systems: plasma alone system, plasma with glass beads in the discharge zone and plasma with catalyst (Pt-Re/Al_2O_3) in the discharge zone. Conversion of 100% was achieved in the plasma with glass beads system at low feed rate (20 mL/min), while at high feed rates (50 mL/min) the plasma-catalytic system had the best performance, achieving 90% conversion. The maximum energy efficiency (26.1%) was achieved in the plasma alone system. Finally, the authors concluded that high carrier gas flow (50 mL/min) and low discharge power (< 10 W) boost CH_4 conversion and suppress coke formation.

Górska et al. [84] fed CH_4, H_2 and Ar in a DBD reactor at 1.2 bar and 240 °C and investigated the effect of presence of packing material inside the plasma zone on the reaction performance. For this purpose, neutral quartz glass beads were placed inside the discharge. CH_4 conversion was 21.4%, without the presence of packing and 22.7% when using quartz glass beads; thereafter, a stationary catalytic bed of Cu/ZnO/Al_2O_3 replaced the quartz glass beads. CH_4 conversion was 21.7% for the first 4.5 h, but decreased to 16.7% after 81.5 h. In all cases, C_2 hydrocarbons were formed, but in case of catalyst use, no C_2H_2 was produced. However, selectivity to C_2 was maximized in the presence of catalyst and minimized in the case of plasma alone. Kasinathan et al. [85] tested various catalytic materials to enhance CH_4 conversion and product selectivity (mainly C_2H_2, C_2H_4 and C_2H_6) in a DBD reactor at ambient pressure and temperature. Four different catalysts were used: Al_2O_3, MgO/Al_2O_3, TiO_2/Al_2O_3 and SiO_2; the results were compared with the plasma discharge without catalyst and the following results were obtained; plasma without catalyst: CH_4 conversion 7.2%, Al_2O_3: CH_4 conversion 10.4% (discharge power 4.18 W, 201 m^2/g), MgO/Al_2O_3: CH_4 conversion 16.2% (discharge power 3.60 W, 184 m^2/g), TiO_2/Al_2O_3: CH_4 conversion 14.1% (discharge power = 3.36 W, 212 m^2/g), SiO_2 (comparable conversion to plasma without catalyst). C_2, C_3 and C_4 hydrocarbons were formed as products.

However, the catalytic material is not the only factor, which influences CH_4 conversion and product selectivity. The physical characteristics of the catalyst may induce changes in the electric field too. Therefore, Kasinathan et al. [85] also studied the impact of MgO/Al_2O_3 particle size on the reactor performance. Smaller particles increased the surface interactions between the catalyst and the reaction species resulting in higher conversion and changes in product selectivity. Particularly, CH_4 conversion increased with decreasing catalyst size from 1.75 mm to 0.25 mm. C_2 and C_3 product distribution was also affected by the particle size; particularly, selectivity to C_2H_6 and C_3H_8 decreased significantly with decreasing catalyst size, but selectivity to C_2H_2 increased with decreasing catalyst size. Selectivity to C_2H_4 and C_3H_6 slightly increased with smaller catalyst particles. Jo et al. [86] investigated the surface area and the catalyst shape impact on discharge characteristics in order to develop better materials that can be used as catalytic supports in plasma-catalytic hybrid systems. For this purpose, they studied CH_4 conversion in a planar-type DBD reactor using γ-Al_2O_3 (porous spheres of 1 mm diameter with large surface area of 151.3 m^2/g), α-Al_2O_3 (non-porous spheres of 1 mm diameter with low surface area of 1 m^2/g) and crushed γ-Al_2O_3 (0.85–1.13 mm) with sharp and random geometries. The number of micro discharges and the discharge period were the same for γ-Al_2O_3 and α-Al_2O_3 but the electric current (so as the electron density) was higher in γ-Al_2O_3 (Fig. 7). At identical conditions, conversion for γ-Al_2O_3 was the highest (18.3%) at applied voltage of 6 kV and 14.2 W discharge power. Similar CH_4 conversion was obtained for porous spheres and crushed γ-Al_2O_3; however, the

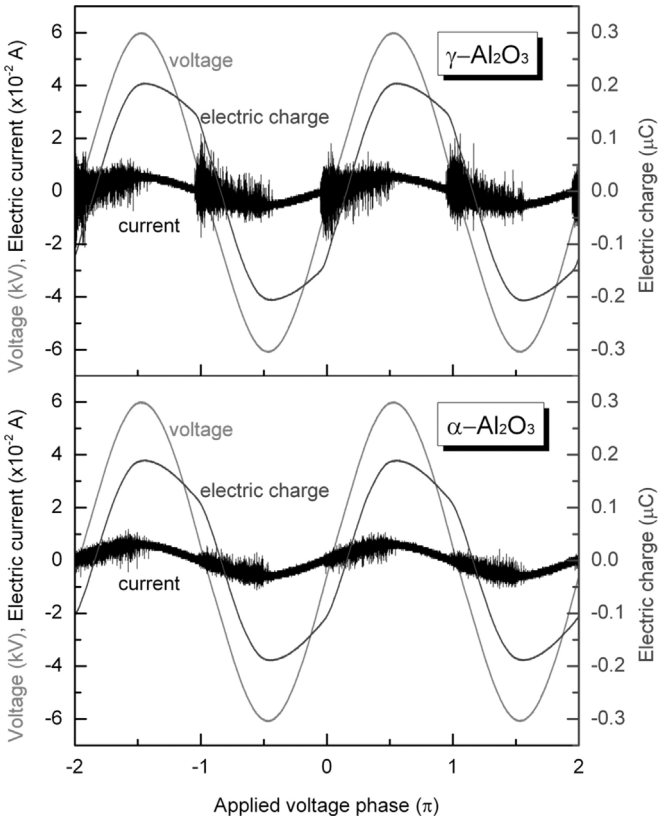

Fig. 7. Applied voltage, current, and electric charge waveforms in CH_4–Ar DBD with γ-Al_2O_3 and a-Al_2O_3 bead packing.
Reproduced with permission from Jo et al. (2013).

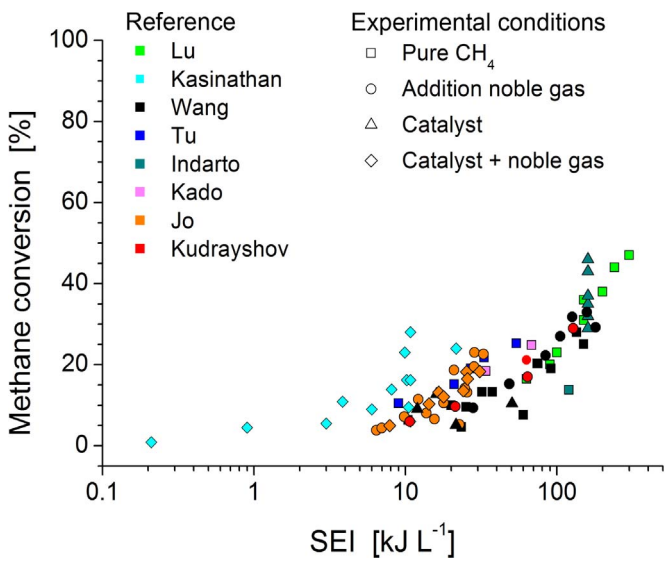

Fig. 9. Methane conversion vs SEI in DBD reactors. The most promising results have been selected from the following references; Lu et al. [69], Kasinathan et al. [85], Wang et al. [70,81,88], Tu et al. [71], Indarto et al. [49], Jo et al. [78–80], Kudrayshov et al. [89] and Kado et al. [90].

breakdown voltage of crushed γ-Al_2O_3 was higher than both porous spheres of γ-Al_2O_3 and α-Al_2O_3. The breakdown voltages for porous spheres of γ-Al_2O_3 and α-Al_2O_3 were similar.

Differences in the surface of α-Al_2O_3 and γ-Al_2O_3 affected the discharge characteristics, such as electron density and electron temperature. Not only the physical, but also the electrical properties of the catalytic material may affect the discharge characteristics. It was proven by Jo et al. [87] that high electric conductivity impoverishes the electric field; therefore the electron density and electron temperature drop, reducing thus CH_4 conversion. Bare γ-Al_2O_3 and Pt/Al_2O_3 (1 mm diameter 151.3 m^2/g BET surface for both samples) were used for the experiments. It was noticed that conversion of CH_4 using Pt/Al_2O_3catalyst was lower than γ-Al_2O_3. The presence of Pt distorted the electric field and resulted in weaker electric field (Fig. 8). The selectivity to C_2H_6 was higher but the selectivity to C_2H_2 was lower in Pt/Al_2O_3 as compared to γ-Al_2O_3. This fact confirms that the electric field strength decreased in the presence of a conductive catalyst because the population of CH increases under strong electric field conditions; in contrast, CH_3 concentration increases under weak electric field conditions. As C_2H_6 is generated by recombination of CH_3 radicals, and C_2H_4 by CH radicals, a weak electric field boosts C_2H_6 formation, whereas a strong electric boosts C_2H_4 formation.

4.1.2. Analysis of the performance

The most promising results for non-oxidative methane coupling that have been achieved with a DBD reactor are presented in Figs. 9 and 10. A fair evaluation of different experimental setups performance is rather difficult because essential information is missing and the reported data are often incomplete or incoherent. For instance, the reported power input sometimes corresponds to the deposited power into the plasma and sometimes to the consumed power by the generator. This may induce important errors in energy efficiency calculations and eventually to overestimation/underestimation of the setup performance. However,

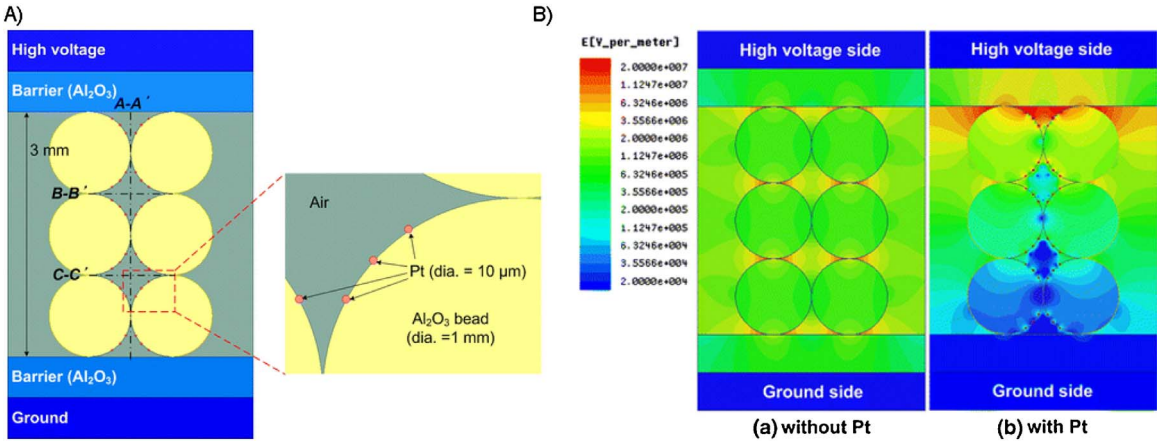

Fig. 8. (A) schematic diagram for electric field calculation of DBD reactors packed with Al_2O_3 beads with and without Pt. (B) modelling results of electric field distribution inside the DBD reactor packed (a) with the Al_2O_3 beads without Pt and (b) with the Al_2O_3 beads with Pt.
Reproduced with permission from Jo et al. (2014).

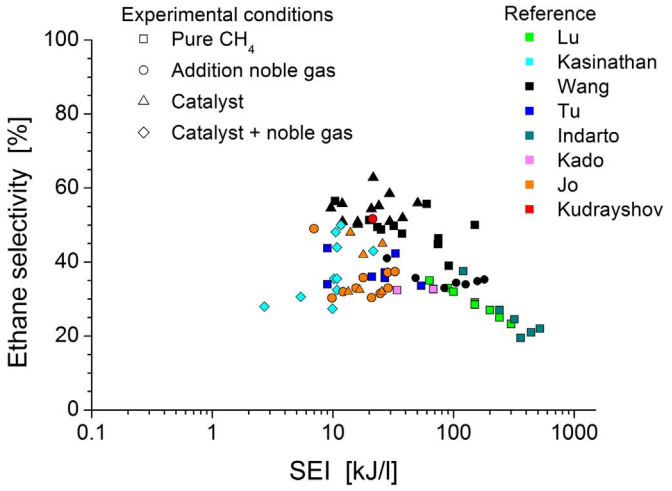

Fig. 10. Ethane selectivity vs SEI in DBD reactors. The most promising results have been selected from the following references; Lu et al. [69], Kasinathan et al. [85], Wang et al. [70,81,88], Tu et al. [71], Indarto et al. [49], Jo et al. [78–80], Kudrayshov et al. [89] and Kado et al. [90].

some general trends can be concluded.

In Fig. 9, the conversion of CH_4 over the specific energy input (deposited into the plasma zone) is presented while in Fig. 10 the ethane (C_2H_6) selectivity over the specific energy input is presented. It can clearly be seen that SEI increase results in higher conversion and lower selectivity to C_2H_6. Noble gas addition also increases CH_4 conversion and decreases selectivity to C_2H_6. However, the noble gas effect on the DBD performance is weak and considering its high cost, it cannot be a viable solution in industrial processes. Catalyst use changes the nature of the discharge and influences the performance. The catalyst impact depends on the nature of the catalyst. Although catalysts commonly increase C_2H_6 selectivity in DBD reactors, their effect on CH_4 conversion is not always qualitatively consistent; i.e., both increasing and decreasing CH_4 conversion trends have been reported when a catalyst is placed in the discharge zone. Therefore, fit-for-purpose catalysts, tailored to integration with plasma discharges, need to be developed.

4.2. Gliding arc (GA)

A gliding arc is initiated between two coplanar diverging electrodes and the gas flow propels the thin plasma arc along the edges of those electrodes. When the length of the gliding arc exceeds its critical value, the heat losses surpass the energy supplied by the source and it is not possible to sustain the plasma in thermodynamic equilibrium. As a result, a fast transition from thermal into non-equilibrium plasma occurs [91]. GA shows promising results for fuel reforming applications, with low specific power consumption and high energy efficiency compared to other non-thermal plasma reforming processes because endothermic chemical reactions can be enhanced by absorbing up to 80% of the electrical energy provided by the arc discharge [91]. However, only 10–15% of the gas flow comes into contact with the arc and experiences very short residence time inside the plasma [92]. To prolong the contact time between the input gas flow and plasma, the following approaches have been adopted. A reverse vortex flow reformer was studied in [93,94]; this configuration thrusts an arc to sweep a three dimensional space creating higher plasma volume (Fig. 11); that way, the residence time increases within the plasma enabling uniform gas treatment. A mini-gliding arc [95] has been used as another effective configuration in which most of the reactor volume is occupied by the plasma; low gas flows ensure high contact time between the gas and the discharge.

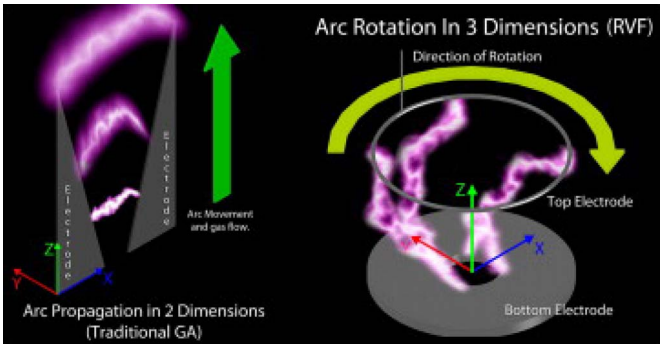

Fig. 11. left: typical 2-dimensional gliding arc; right: 3-dimensional arc propagation in a reverse vortex flow.
Reproduced with permission from Piavis et al. (2015).

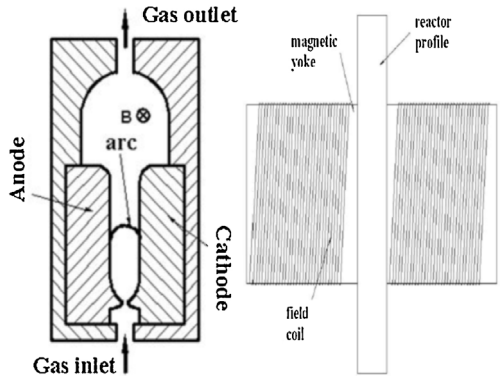

Fig. 12. Schematic representation of a GA reactor.
Reproduced with permission from Yuhan et al. (2007).

Dae Hoon et al. [96] developed a rotating arc reactor and studied the influence of the arc length on C_2 selectivity. They employed two different plasma reactor geometries: a conical electrode, which was much shorter than the outer cylindrical electrode (Reactor I) and a conical electrode, which was slightly longer than the outer cylindrical one (Reactor II). For the same specific energy input, the arc length was longer in Reactor I but the authors have not drawn any conclusion regarding C_2 selectivity due to its complicated dependence on arc length. A completely different and unique way to control the plasma was reported by Yuhan et al. [97] who tested CH_4 reforming to C_2H_2 in a GA reactor under the influence of a magnetic field. To attain this, the whole gliding arc reactor system was placed between two magnetic yokes (Fig. 12). The magnetic field was perpendicular to the plane where the electrodes were placed. The arc was periodically moving upward forced by the feed flow and Lorenz force. Specific energy input (varied with feed flow rate) and magnetic field intensity were the studied parameters, which both affected CH_4 conversion and C_2H_2 selectivity. Specifically, the highest CH_4 conversion and C_2H_2 selectivity were 68% and 80%, respectively, and were attained at 0.8 T and 11.7 kWh/m^3.

Hu et al. [98] performed CH_4 reforming in the presence of Ar in a GA. CH_4/Ar ratio, CH_4 flow rate, input voltage and minimum electrode gap were varied to investigate their effects on CH_4 conversion and product distribution. As Ar content increased, CH_4 conversion as well as C_2 and H_2 selectivity increased because the Ar metastable state enhanced electron impact reactions. When CH_4 flow rate increased, the residence time and the specific energy input decreased thus decreasing the probability of collisions between CH_4 molecules and high energetic electrons. Hence, CH_4 conversion and H_2 selectivity decreased while C_2 selectivity remained almost constant. Conversion of CH_4 increased almost linearly with input voltage increase as it had already been mentioned in previous works. Minimum gap increase led to higher residence time and reaction volume, thus, CH_4 conversion, C_2

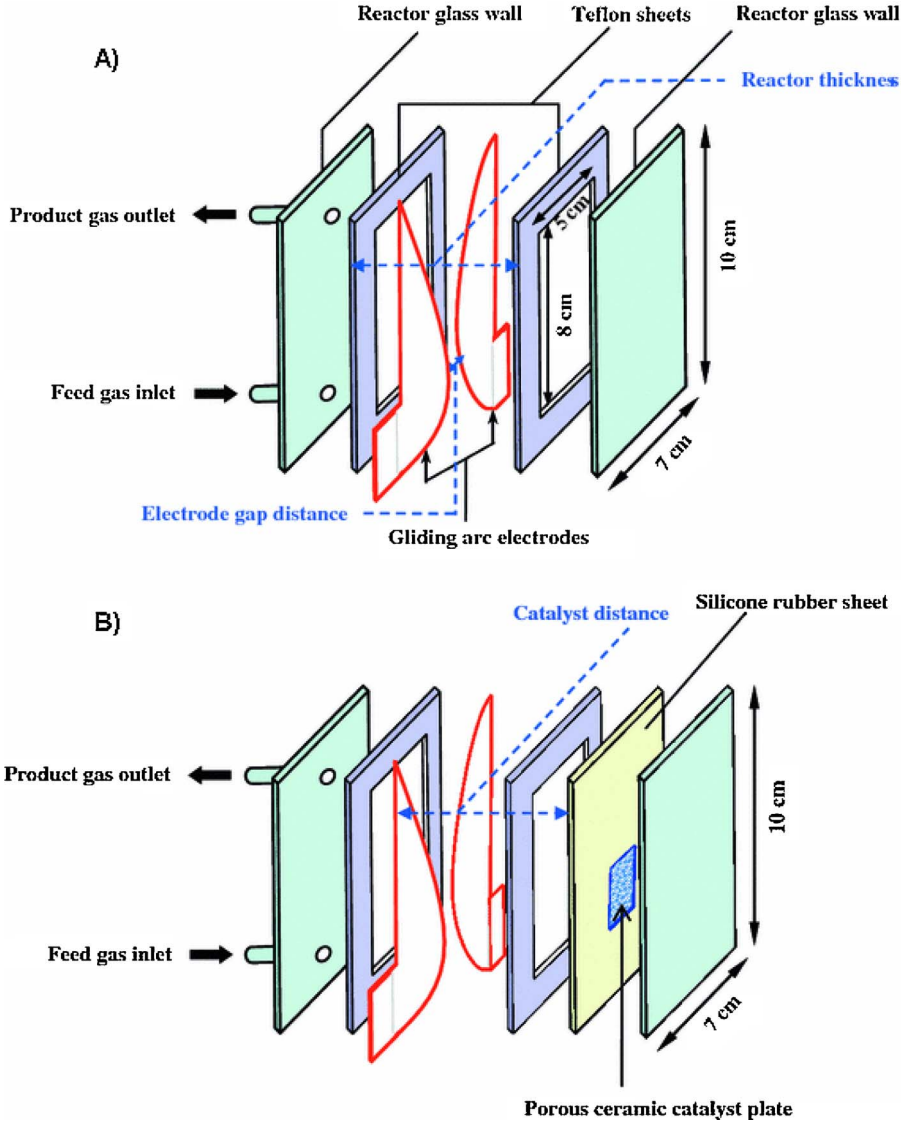

Fig. 13. Configuration of a mini-gliding arc discharge reactor: (A) without catalyst and (B) with catalyst.
Reproduced with permission from Rueangjitt et al. (2011).

and H_2 selectivity increased.

Zhang et al. [99] developed an atmospheric pressure rotating gliding arc discharge co-driven by a magnetic field and tangential flow to study CH_4 reforming to H_2. To enhance CH_4 conversion, N_2 was co-fed with CH_4 in the discharge. The discharge was characterized by means of optical emission spectroscopy; mainly CN, C_2, and CH radicals were detected. The maximum CH_4 conversion was 91.8% at a flow rate of 6 L/ min and CH_4/N_2 ratio of 0.1. The major product was H_2 and the highest H_2 selectivity was 80.7% at the same flow rate (6 L/ min) and CH_4/N_2 ratio of 0.05. Since carbon deposition affected the continuous operation of the RGA discharge, a resistance of 40 kΩ, CH_4/N_2 ratio in the range of 0.1-0.4 and flow rate of 8 L/min were recommended as optimum operating conditions.

4.2.1. Integration of plasma-catalytic reactions

The synergistic effect of the hybrid plasma-catalytic system has been examined in gliding arc reactors. Two different configurations for the catalyst placement have been studied: a spouted catalyst placed inside the plasma zone and a fixed catalyst bed placed downstream of the plasma. The advantages and disadvantages are described in the respective papers.

Rueangjitt et al. [100] studied CH_4 reforming in a mini-gliding arc discharge (Fig. 13A). The concentration of CH_4 in Ar flow, feed flow rate, electrode gap and presence of catalyst bed past the plasma zone were the investigated parameters. Conversion of CH_4, H_2 and C_2 yields decreased with increasing amount of CH_4 in the feed due to lower Ar heat capacity; Ar concentration decrease leads to lower temperature in the plasma zone and, therefore, CH_4 conversion drops. Increase in feed flow rate reduced the residence time and the power density, mitigating the possibility of electron-molecule collisions and so, CH_4 conversion was reduced, but the selectivity got only slightly affected. However, the shorter residence time and the lower energy of electrons resulted in lower carbon formation. Discharge gap increase led to weaker electric field (lower energy electrons generation) and higher discharge volume (reaction volume). The overall CH_4 conversion and product yields increased indicating the domination of residence time over the electric field strength. The hybrid plasma-catalytic system (Fig. 13B) was also tested and compared with the plasma alone configuration. The hybrid system demonstrated higher performance under any operating conditions, which was attributed to the interaction of the excited species in the plasma zone with the Ni-loaded catalyst. The distance of catalyst from the discharge was found to be a critical factor determining the reactor performance. The shorter the distance, the higher the probability of the excited species to interact with the catalyst; long distance

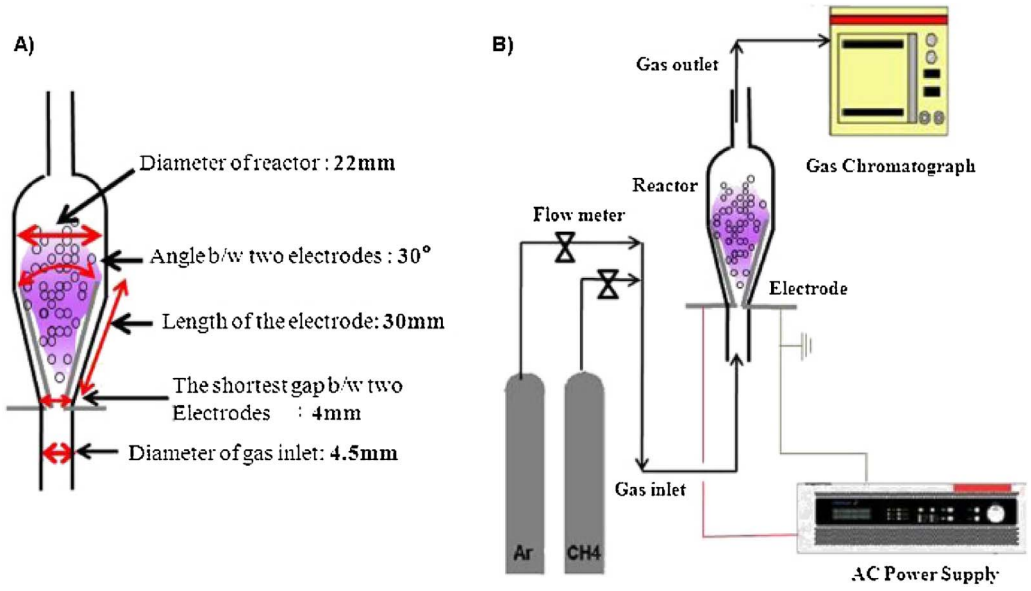

Fig. 14. (A) configuration of the gliding arc discharge reactor; (B) experimental setup. Reproduced with permission from Lee and Sekiguchi (2011).

between the discharge and the catalyst allows for relaxation of the excited species to the neutral state.

Instead of a catalytic bed, Lee and Sekiguchi [101] used a hybrid system of a gliding arc with spouted catalytic bed to investigate the effect of different catalysts on the reaction performance (Fig. 14). Catalytic materials such as Pt/Al_2O_3, Pd/Al_2O_3, Rh/Al_2O_3, Ru/Al_2O_3 and Al_2O_3 particles were used in the experiments. The difference in CH_4 conversion was negligible among the catalysts. However, CH_4 conversion in plasma alone discharge was always higher than the hybrid plasma catalytic system. This observation is contradictory to Rueangjitt and his co-workers' results. Lee and Sekiguchi reported that discharge distortions imposed by the spouted catalyst inside the plasma zone was the main reason for the low conversion. Use of Pt/Al_2O_3 and Pd/Al_2O_3 catalytic materials promoted C_2H_4, C_2H_6 and C_2H_2 while use of Ru/Al_2O_3 and Rh/Al_2O_3 promoted C_2H_2, H_2 and soot. The performance of all the catalysts decreased over the reaction time; however, Pd/Al_2O_3 showed the highest resistance to deactivation.

Schmidt-Szalwoski et al. [102] also focused on a hybrid system of a gliding arc with spouted catalytic bed to improve CH_4 coupling and compare the reaction performance with the plasma alone system. Two catalysts were examined: Pd and Pt supported on Al_2O_3 particles. The main products for both systems (with and without catalyst) were C_2 and H_2. The distinct effect of catalyst addition was the enhancement of C_2H_6 and C_2H_4 formation. The Pd-based catalyst resulted in higher C_2H_6 and C_2H_4 formation, as compared with the Pt-based one, at low energy input. At high energy input, the Pt-based catalyst was found to perform better though. Further, considerable suppression of soot formation and increase in C_2 selectivity were observed when the catalytic materials were used, as compared with the plasma alone case.

4.2.2. Analysis of performance

The most encouraging results by means of CH_4 conversion and C_2H_2 selectivity as function of specific energy input (SEI) that have been obtained in a GA discharge are presented in Figs. 15 and 16. It is concluded that CH_4 conversion increases linearly with SEI increase. However, selectivity has a broad distribution without a clear tendency, perhaps due to the different experimental conditions applied (e.g.

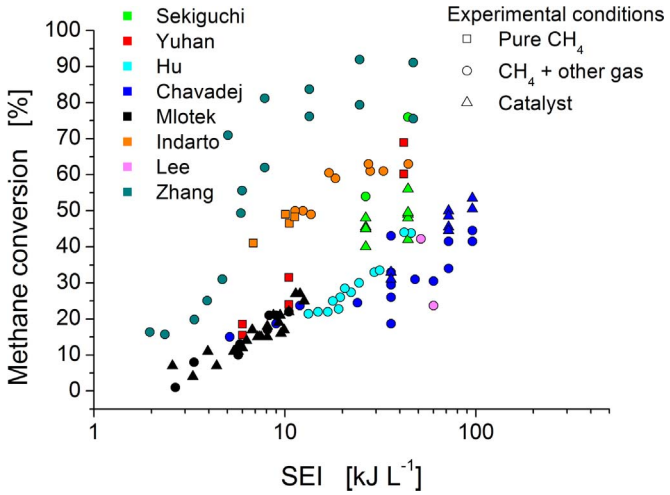

Fig. 15. Conversion of CH_4 in gliding arc discharges as function of the specific energy input (SEI). The most promising results are presented in Sekiguchi et al. [101], Yuhan et al. [97], Hu et al. [98], Chavadej et al. [95,100], Młotek et al. [103,104], Indarto et al. [52,105], Lee et al. [106] and Zhang et al. [99].

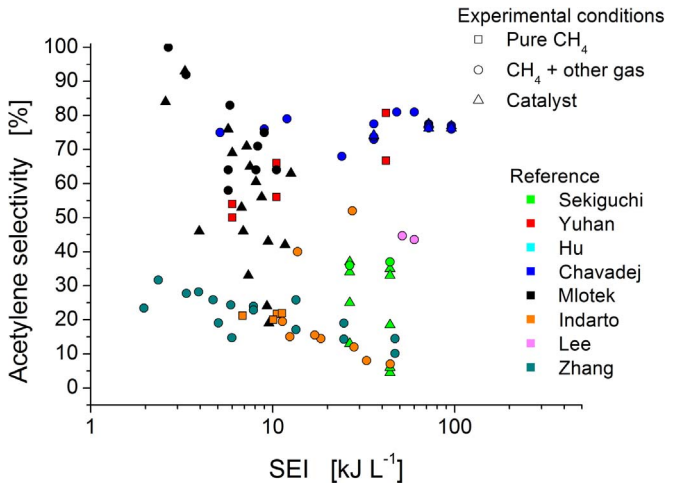

Fig. 16. Selectivity of C_2H_2 in gliding arc discharges as function of the specific energy input (SEI). The most promising results are presented in Sekiguchi et al. [101], Yuhan et al. [97], Hu et al. [98], Chavadej et al. [95,100], Młotek et al. [103,104], Indarto et al. [52,105], Lee et al. [106] and Zhang et al. [99]. However, the selectivity does not show any clear trend as function of SEI, most likely due to the different operating conditions that have been applied in the literature.

residence time). It seems that gas addition faintly increases CH_4 conversion for a given SEI but the effect on selectivity is not clear.

4.3. Corona and spark

Corona discharge is a partial discharge, which is initiated around an active electrode. The restricted ionisation regions that are imposed by the electrode geometry allow high energetic electrons to collide with gas molecules, promoting the electron impact reactions. Corona discharges are scalable and can easily operate under atmospheric pressure [107]. When the input voltage is raised, transitions from corona to glow and finally to spark take place [108]. Glow discharge is an unstable regime; therefore, corona turns almost immediately to spark [109]. As these two regimes have similar configuration, the results for both corona and spark discharge are presented together.

Aleknaviciute et al. [110] worked on CH_4reforming to H_2 at atmospheric pressure and in presence of Ar (CH_4:Ar = 1:1). They studied a pin-to-plate plasma configuration under corona regime. As it had already been studied and observed in previous works, they reported that high input power and long residence time had a positive effect on CH_4 conversion and H_2 selectivity. Moreover, they observed that bigger discharge gaps favour H_2 production. The effect of discharge gap had also been previously studied but a different interpretation is given in Aleknaviciute et al. [110]; specifically, whilst most of the researchers claimed that the reason of CH_4 conversion increase when increasing the discharge gap at constant flow rate is the longer residence time, Aleknaviciute et al. [110] supported Kado's [111] explanation, according to which the breakdown voltage is affected by the discharge gap and the breakdown voltage is the dominant factor rather than the residence time. Particularly, they claimed that the higher breakdown voltage, which is needed as the gap length increases, shifts the electrons energy distribution to higher energy values, which give rise to higher CH_4 conversions. They also tested positive and negative corona and concluded that positive corona led to higher H_2 yields. Conversion of 41% at a discharge power of 19 W and H_2 selectivity of 48% were reported. Beloqui Redondo et al. [112] studied conversion of CH_4 to C_2H_2 in a corona discharge. A pin-to-plate configuration and pure CH_4 were used for the experiments. The highlight of their experiments was the coating of the electrodes with gold to examine whether gold enhances the reaction and suppresses carbon formation. The stability of the reactions was considerably increased after the coating and 28% of CH_4 conversion and 76% of C_2H_2 yield at specific energy requirement of 26.2 kWh/kg C_2H_2 were obtained.

Horvart et al. [113] fed N_2 and CH_4 in a volume ratio of 98:2 in a corona discharge to interpret the results from the Cassini Huygens space mission and provide additional simulation of chemical processes in Titan's atmosphere. Species such as CH, CH_2, CH_3, NH_2, NH, CN and NCN were mainly detected in the discharge and C_2H_2, HCN, C_2H_6 were the main products. A high amount of energy was spent for CH_4 decomposition (2.7 kWh/gCH_4).

Regarding spark discharge, Malik et al. [114] reformed CH_4 and liquid hydrocarbons to H_2 and light hydrocarbons using a pin-to-plate electrode configuration at room and atmospheric pressure in the spark regime. In the case of CH_4 reforming, 2.4 mol of CH_4 were converted per kWh of energy input, producing 1.5 mol H_2, while the production rate of all gaseous products was 0.31 μmol/s. Moshrefi et al. [115] worked on DC spark discharge plasma to produce H_2 and carbon black from CH_4, using a rotating electrode with fast start-up and rapid response. They also studied the effect of current and voltage on reactor performance at various feed flow rates [116]. High voltage and high current resulted in high CH_4 conversion and high H_2 production, but low C_2 selectivity. They observed that variation of ground electrode rotation speed affects the breakdown voltage. Moreover, the authors claimed that high number of electrons (high current) with sufficient energy to activate CH_4 dissociation reactions is preferred, in terms of energy utilization efficiency, to a low number of electrons with high energy. In the second case, when high energy electrons collide with CH_4 molecules, the result is not only molecular dissociation, but also gas heating, due to surplus of energy, which reduces the energy utilization efficiency (Fig. 17).

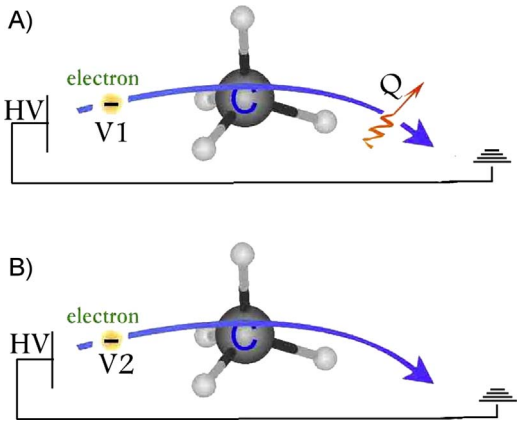

Fig. 17. Schematic presenting the principle of electric energy loss in form of heat at high power and flow rates. (A) Electrons with very high energy result in both methane dissociation and gas heating due to the surplus of energy; (B) Electrons with lower energy (still enough for CH_4 dissociation) result only in methane dissociation.
Reproduced with permission from Moshrefi et al. (2014).

Lotfalipour et al. [47] conducted a complete parametric study of CH_4 conversion using a repetitive nanosecond plasma discharge. The study was focused on the effect of applied voltage, discharge gap, repetition frequency and residence time on conversion and product selectivity. The maximum CH_4 conversion obtained in this work was ~60%, while C_2H_2 was the dominant product (~70% selectivity). The importance of the molecule vibrational excitation forCH_4 dissociation was highlighted and supported by a model according to which the vibrational temperature considerably exceeds the translational temperature at high non-equilibrium molecular state.

Wang and Guan [117] investigated CH_4 reforming to olefins in a two-stage recycle-plasma-catalyst reactor. In the first stage, a mixture of mainly C_2H_2 and H_2 was produced by the pulsed spark discharge. In the second stage, Pd and Ni based catalysts were placed downstream of the discharge to selectively hydrogenate acetylene to ethylene without extra H_2 source; H_2 that was generated by the discharge was used for the hydrogenation reaction. It was observed that plasma reactor reactivity and energy efficiency were enhanced by recycling part of plasma effluent back to the discharge zone. The recycle-plasma-catalyst reactor reached 73% CH_4 conversion at 24 kW in the discharge and 55% and 35% ethylene yield using Pd-based and Ni-based catalysts, respectively. Aside from ethylene, C_3–C_5 light olefins were also formed.

4.3.1. Integration of plasma-catalytic reactions

Wang et al. [118] used a plasma-followed-by-catalyst system to produce C_2H_4 and H_2 from CH_4 in a spark plasma discharge. They reported 80% CH_4 conversion at a discharge power of 32 W and approximately 52% overall C_2H_4 yield using a Pd-Ag/SiO catalyst past the plasma zone.

4.3.2. Analysis of the performance

The best literature results that have been obtained for CH_4 conversion and C_2H_2 selectivity as function of specific energy input (SEI) in corona and spark discharges are presented in Figs. 18 and 19, respectively. These discharges are usually studied in the same setup and sometimes it is difficult to distinguish the plasma regimes. In both cases, CH_4 conversion increases with SEI increase and higher conversions are generally achieved in spark discharges. As far as C_2H_2 selectivity is concerned, a concrete trend is not apparent in Fig. 19. It

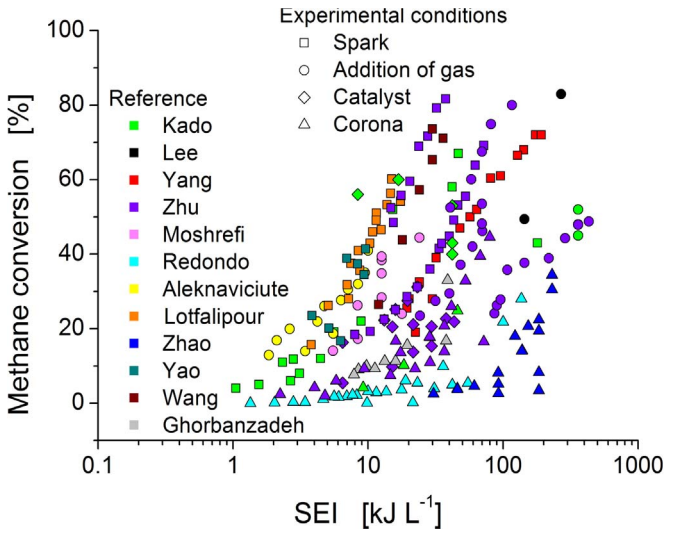

Fig. 18. Methane conversion in corona and spark discharges. The most promising results are presented in Kado et al. [90,111,119], Lee et al. [106], Yang et al. [120], Zhu et al. [88,121–126], Moshrefi et al. [115,116], Redondo et al. [112], Aleknaviciute et al. [110], Lotfalipour et al. [47], Zhao et al. [127], Yao et al. [128], Wang et al. [117] and Ghorbanzadeh et al. [129].

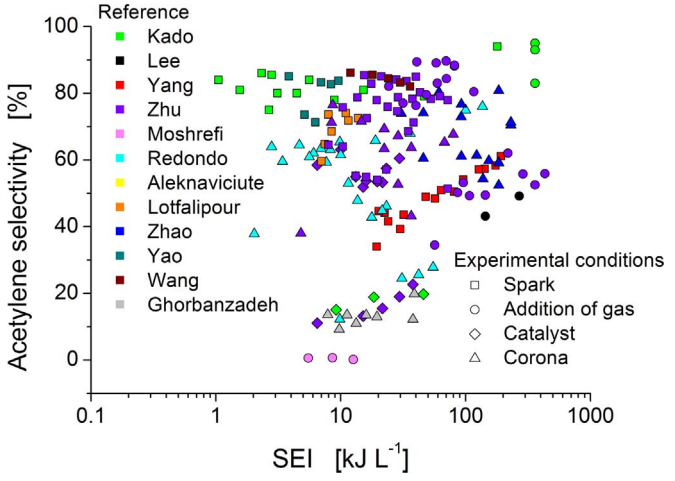

Fig. 19. Acetylene selectivity in corona and spark discharges. The most promising results are presented in Kado et al. [90,111,119], Lee et al. [106], Yang et al. [120], Zhu et al. [88,12–126], Moshrefi et al. [115,116], Redondo et al. [112], Aleknaviciute et al. [110], Lotfalipour et al. [47], Zhao et al. [127], Yao et al. [128], Wang et al. [117] and Ghorbanzadeh et al. [129].

seems however that acetylene selectivity is maximized in spark discharges. Addition of H_2, N_2 and noble gases increase CH_4 conversion (not drastically), but it is not clear what the impact on C_2H_2 selectivity is. Catalyst use may increase both CH_4conversion and C_2H_2selectivity depending on the catalyst properties and position.

4.4. Microwave (MW) discharge

Microwave discharges are initiated and sustained by electromagnetic waves with high frequency (~2.45 GHz). In majority of reactors used for methane conversion microwaves travel through a rectangular waveguide with a reduced height section followed by tapered sections. The plasma is generated inside a cylindrical electrode, which penetrates the waveguide [130]. MW discharges are widely used for generation of quasi-equilibrium and non-equilibrium plasma for different applications and hold significant advantages over other types of electrical discharges, such as simplicity of plasma ignition, wide region of operating pressures (and atmospheric), absence of contamination of gas phase by electrode erosion parts and ability to treat large gas volumes.

Shen et al. [131] investigated CH_4 reforming to C_2H_2 under MW plasma. The maximum conversion they reported was 93.7% at 0.16 bar. The main product formed in the discharge was C_2H_2 and the maximum yield was 88.6% for a specific energy input of 2.43 kJ/molC_2H_2. The rectangular waveguide resonator characteristics and the reaction tube position significantly influenced the performance of the reaction while pressure increase had a minor effect. They also studied the performance of the MW plasma reactor at atmospheric pressure [132] focusing on the effect of the CH_4:H_2 molar ratio, flow rate and MW power. They observed that H_2 had a positive twofold effect; carbon formation was supressedandCH_4conversion and C_2 yield increased. Feed flow rate increase lowered CH_4 conversion,C_2 selectivity and carbon formation. Higher conversion and C_2 yield were obtained when the MW power was increased.

Mizeraczyk et al. [133] employed atmospheric MW plasma for gas processing applications. Among the applications, H_2 production via CH_4 reforming was also considered. They managed to produce up to 0.11 kg/h of H_2 at a CH_4 feed flow rate of 175 L/min and specific energy input of 96 kJ/molH_2.

Jasínski et al. [134] produced H_2 via CH_4 conversion using atmospheric MW plasma. Gases were introduced in the plasma by four gas ducts creating swirl flow, which was concentrated near the quartz cylinder wall and stabilised plasma generation. H_2 and carbon were the main products. The production of H_2 reached 0.87 kg/h at a feed flow rate of 212 L/min and input power of 5 kW. In another work [135] of the same group, the authors developed two types of atmospheric MW plasma reactor namely, a nozzleless waveguide-supplied coaxial line-based reactor and a nozzleless waveguide-supplied metal cylinder-based reactor (Fig. 20). N_2 and CO_2 were used as swirl flow gases. The optimal results obtained concerning H_2 production rate and specific

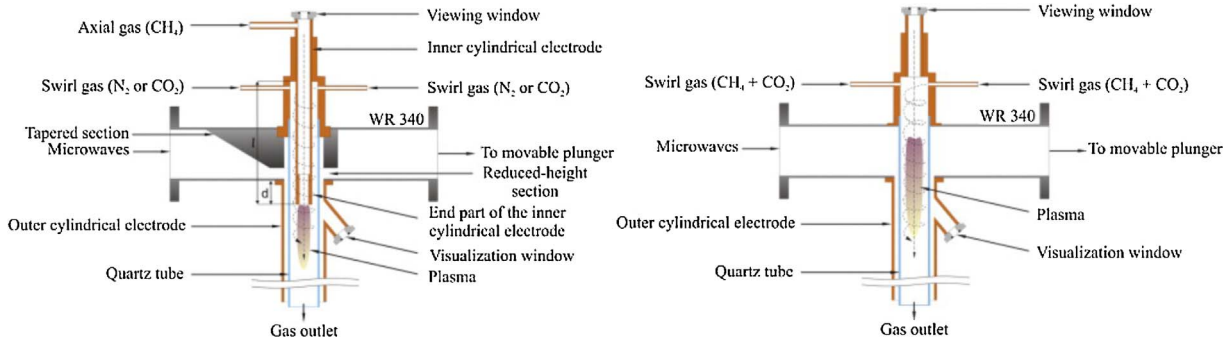

Fig. 20. On the left the schematic view of the nozzleless waveguide-supplied coaxial line-based microwave plasma source; on the right the schematic view of the nozzleless waveguide-supplied metal cylinder-based microwave plasma source.

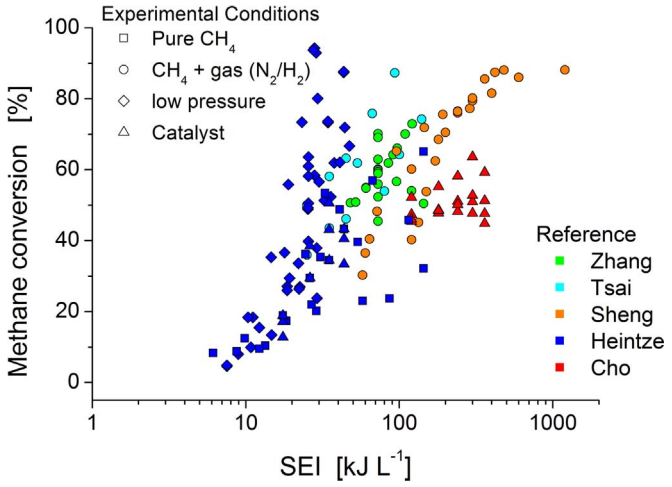

Fig. 21. Methane conversion in MW discharges. The most promising results are presented in Zhang et al. [136], Tsai et al. [137], Shen et al. [132], Heintze et al. [138–140] and Cho et al. [141].

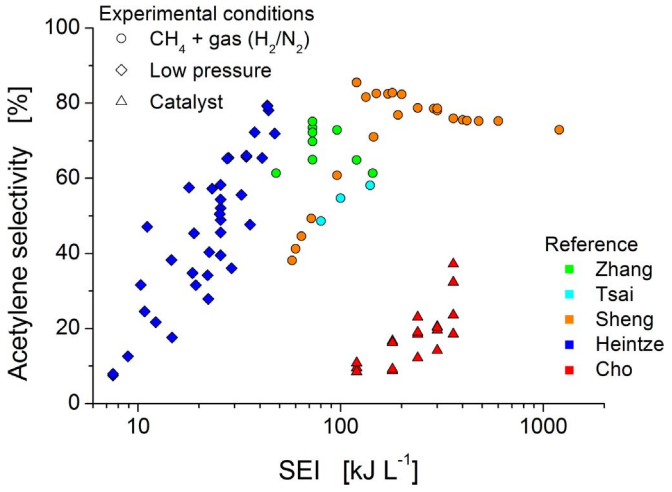

Fig. 22. Acetylene selectivity in MW discharges. The most promising results are presented in Zhang et al. [136], Tsai et al. [137], Shen et al. [132], Heintze et al. [138–140] and Cho et al. [141].

energy input were 0.05 kg/h and 403.2 kJ/molH_2, respectively, with the first reactor, and 0.098 kg/h and 230 kJ/molH_2, respectively, with the second reactor.

4.4.1. Analysis of the performance

The most positive literature results regarding CH_4 reforming in terms of CH_4 conversion and C_2H_2 selectivity as function of the specific energy input (SEI) are presented in Figs. 21 and 22. It is obvious that SEI increase results in higher CH_4 conversion. Addition of inert gases has a positive effect on the conversion rate. The same trend is observed for the catalyst use too. In addition, low operating pressure significantly increases CH_4 conversation. Selectivity to C_2H_2 increases with SEI increase up to a certain value. Once SEI exceeds a critical value (200 kJ/L_{CH4}), C_2H_2 selectivity drops. This local maximum of C_2H_2 selectivity can be explained by the different products that are formed at different SEIs. Particularly, ethane is the favourable product at low SEI; as SEI increases, acetylene becomes the favourable product; when SEI increases further, carbon formation reduces the selectivity to C_2H_2.

4.5. Other works

Besser and Lindner [142] developed microplasma reactors (reactors with micro-hollow cathode discharge structure) to investigate CH_4 reforming (Fig. 23). N_2 was co-fed with CH_4 to enhance CH_4 conversion through the Penning ionization phenomenon [66]. The conversion of CH_4 reached 22.8% and carbon was the major product (64.7% selectivity); acetylene (C_2H_2) and ethane (C_2H_6) were also formed at 23.5% and 11.8% concentration, respectively, at molar base.

A new rotary multidentate helix electrode was constructed and used by Wang et al. [143] to study plasma-assisted natural gas conversion to C_2 hydrocarbons at atmospheric pressure in the presence of H_2. Applied voltage and feed flow rate were the varied parameters. A significant difference in reaction performance was observed when the applied voltage overpassed the value of 2.4 kV; the C_2 single pass yield increased from 69.85% to 75.66%, and CH_4 conversion increased from 70.46% to 77.31%.Coke formation was also detected on the electrode surface and reactor walls. This remarkable change in the performance was explained by the plasma regime transition from glow to arc.

Lee et al. [106] used different plasma sources (AC and pulsed DBD, AC and pulsed spark, hollow cathode, gliding and rotating arc) to compare CH_4 activation under identical conditions. They observed that plasma sources with high degree of warmness, such as spark, hollow cathode and arc, yield higher CH_4 conversion and higher C_2H_2 and H_2 selectivity. On the contrary, the DBD plasma source resulted in low CH_4 conversion, as the degree of warmness is very low, and ethane was obtained as major product. The AC spark plasma source gave the best performance in terms of methane conversion (~83%) and product selectivity (~49% C_2H_2).

Ghorbani et al. [144] used a nanosecond laser to generate plasma and assist the catalytic CH_4 decomposition. Various metal-based catalysts were tested: Ni, Fe, Pd, and Cu. Components such as H_2, C_2H_2, C_2H_4, C_2H_6, C_3H_6, and C_3H_8 were mainly formed but varied considerably from metal to metal. However, CH_4 conversion was very low for all the metals and never exceeded 2.2%. Ding et al. [145] initiated non-equilibrium pulsed discharges inside the liquefied natural

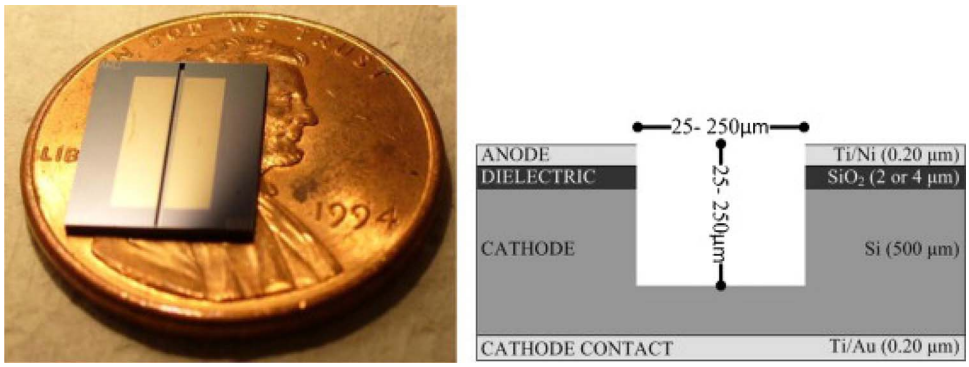

Fig. 23. The microplasma reactor chip (relation to US one cent coin) and the schematic cross-section of microplasma reactor chip; key layers and critical dimensions of the device are shown.
Reproduced with permission from Besser and Lindner (2011).

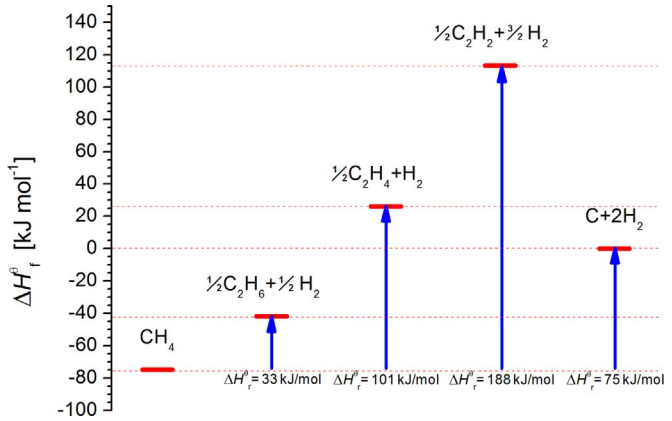

Fig. 24. Methane coupling reactions. All reactions are endothermic; acetylene formation reaction has the maximum enthalpy of formation.

gas (LNG) to study the direct conversion of LNG to syngas and ethylene. Ethylene selectivity was high (97%) but CH_4 conversion was not satisfactory (only 2.3%).

Yu et al. [146] developed a discharge where ionic liquids (ILs) covered the grounded electrode. They prepared nine different imidazolium-based ILs and they used them for CH_4reforming in presence of H_2 (H_2:CH_4 = 0.6:0.4 volumetric ratio) under DC discharge conditions at atmospheric pressure. They observed that the conductivity and viscosity of the prepared ILs influenced the performance of the discharge and particularly viscosity was crucial for the stability of the gas-liquid interfacial plasma. The main products were C_2H_2, C_2H_4, C_2H_6, H_2, and traces of C_3—C_4 hydrocarbons. The highest CH_4 conversion (~44%) was reached when $C_6MIMHSO_4$ was used as IL. Use of C_6MIMBF_4 and C_6MIMCF_3COO resulted in the highest selectivity (~91%) and the highest C_2 yield (~29%), respectively. Finally, the acidity of the anions was important to explain this behaviour; probably, H^+ protons attract the radicals produced in gas phase and promote CH_4 conversion. Zhang et al. [147] prepared a more complex catalyst. They immobilised Pd and C_6MIMBF_4 on γ-Al_2O_3 (Pd-IL/γ-Al_2O_3) and explored the catalytic activity for CH_4 reforming to ethylene inside the plasma. Methane conversion and ethylene selectivity were ~41% and ~62% respectively for 40% C_6MIMBF_4 loading (on mole base) and 20.4 W power input.

5. Comparison among all plasma techniques used for methane coupling and benchmarking with thermal energy-driven methane coupling

Numerous plasma-assisted processes have been investigated and proposed for direct CH_4 reforming to added value products. A fair comparison of all those processes is not easy. Different target products, inaccuracies in the analytic techniques that are employed to analyse product streams and calculate the energy consumption, as well as missing information and incomplete literature data (i.e. lack of carbon and H_2 balance) may induce significant errors in the calculations, resulting in over/under estimations and wrong conclusions.

A first evaluation can be made considering only the major products. In case of CH_4 reforming, C_2 compounds (ethane, ethylene and acetylene), carbon and hydrogen are the main products obtained. The energetic thresholds of the main formation reactions are shown in Fig. 24. For the sake of simplicity, heavier products (C_3 and higher hydrocarbons) can be excluded as they are formed in low concentrations as compared with the C_2 products (relative selectivity lower than 5–10%).

The global CH_4 coupling reaction can be expressed as following:

$$CH_4 \rightarrow \alpha\ C_2H_6 + \beta\ C_2H_2 + \gamma\ C_2H_2 + (1 - 2\alpha - 2\beta - 2\gamma)\ C_{(s)} + (2 - 3\alpha - 2\beta - \gamma)\ H_2 \quad (29)$$

where CH_4 represents the converted methane; α, β, γ are the reaction coefficients calculated by the product stream analysis and carbon and hydrogen are obtained by mass balance calculations rather than by direct detection. The enthalpy of the global CH_4 coupling reaction depends only on C_2 compounds coefficients and can be expressed as following:

$$\Delta H_r^{\Theta} = 2\ (33.02\ \alpha + 101.12\ \beta + 188.27\ \gamma) + 74.87\ (1 - 2\alpha - 2\beta - 2\gamma)\ [\text{kJ mol}^{-1}] \quad (30)$$

The specific energy input (SEI) is expressed as:

$$SEI = 1345 \times \text{Power [W]/Flow } CH_4\ [\text{mL min}^{-1}]\ \ [\text{kJ mol}^{-1}] \quad (31)$$

For the specific energy input (SEI) calculation, the deposited power into the discharge and the total methane feed flowrate are considered.

The specific energy requirement (SER) is the energy required for full conversion of one CH_4 mole and is expressed as:

$$SER = SEI/\text{Conversion}\ [\text{kJ mol}^{-1}] \quad (32)$$

The efficiency (η %) is expressed as:

$$\eta\ \% = 100 \times \Delta H_r^{\Theta}/SER. \quad (33)$$

The energy requirement (ER) is the energy required for production of one C_2H_2 mole and it is expressed as:

$$ER = 2 \times SEI/(\text{Conversion} \times \text{Main Product Selectivity})\ [\text{kJ mol}^{-1}] \quad (34)$$

Considering the reported experimental results, there are three possible cases:

1. Acetylene is formed as main product in high energy discharges (GA, MW and spark).
2. Carbon is obtained as main product under specific conditions in the discharge.
3. Ethane is obtained as main product (in the case of DBD).

In the first and second case, the calculated carbon amount also includes the amount of C_3 or higher hydrocarbons (generally unsaturated). Consequently, the calculated values of reaction enthalpy and efficiency, based on the equations above, may be slightly underestimated. In the third scenario, the calculated carbon amount contains mainly saturated C_3 or higher hydrocarbons and the calculated values will be slightly overestimated. In Table, the experimental data that correspond to the highest efficiency and lowest specific energy requirement from all methane coupling processes with each plasma technique are presented.

Thermal arc plasma is the only process, which has industrially been applied for CH_4 coupling (Hüels process [57]). In this process, all species (ions, electron and molecules) are at thermal equilibrium; thus it can be considered as a conventional thermal process. It has been especially developed for acetylene (higher value product) and carbon production. The acetylene reaction formation is:

$$2CH_4 \rightarrow C_2H_2 + 3\ H_2, \quad \Delta H = 376\ \text{kJ/mol} \quad (35)$$

The Hüels process comprises a 1.2 m long arc, with power of 8 MW and flowrate of 2344 $\text{Nm}^3\,\text{h}^{-1}$. The products are mainly acetylene (yield ~50%), hydrogen and ethylene and carbon. Right after plasma cracking, quenching takes place to maximize the acetylene/ethylene production and reduce carbon formation. Carbon formation is not totally avoidable and generally decreases the efficiency and increases the energy cost for acetylene production. Carbon synthesis is favoured at longer reaction times (ethylene 10^{-6}–10^{-5} s, acetylene 10^{-4}–10^{-3} s and carbon 10^{-3} s) so a quench rate of $5{\cdot}10^6$ K/s is required. Water or hydrocarbons are used as quenching medium. At the aforementioned

Table 1
Comparison of the best results of all plasma-driven methane coupling processes. Specific energy input (SEI), specific energy requirement (SER), efficiency (η%) and energy requirement (ER) are calculated to facilitate a fair comparison. At atmospheric pressure, arc thermal plasma [57,148] and non-thermal pulsed discharge [128] have the highest performance in terms of efficiency (η %) and energy requirement (kJ/mol_{C2H2}). At lower pressures, MW plasma has demonstrated the highest efficiency (η %) and lowest energy requirement [149].

Technique	SEI [kJ mol^{-1}]	Conversion [%]	Selectivity (Carbon) [%]			SER [kJ mol^{-1}]	$\eta_{calculated}$[%] ($\eta_{reported}$[%])	ER C_2H_x [kJ $mol^{-1}{}_{C2H2}$]	Ref.
			C_2H_6	C_2H_4	C_2H_2				
Arc (Hüels process)	275.4	70.5	–	4.5 [17]	72.9	391	40.5	1080	[57]
Arc (Polak)	310.9	86	–	3.23	88.4	362	48.7 (46)	818.3	[148]
DBD	201.7	10.5	34	19 (C_2H_2 + C_2H_4)		1921	3.4	–	[71]
DBD + catalyst	60.5	6.2	28	36	29	976	10.8	6731	[85]
Corona	194	8.5	–	–	76.5	2278	7.1	5957	[121]
Corona + catalyst	145	4.5	6.6	6.4	58.5	3228	4.4	11034	[124]
PD (Spark)	86.0	23.5	1.9	5.4	85	365	46.9	860	[128]
MW	1076	50.7	–	11.5	61.4	2122	6.9	6920	[136]
MW (30 mbar)	617.0	93.7	1.8	9.8	65.3	659	22.9	2018	[138]
MW (107 mbar)	256.6	–	–	–	85 (Yield)	–	(61)	604	[149]
GA (from NG)	118	21	–	6.4	63	562	17.6	1780	[150]
GA (from CH_4)	115.3	15	2.9	8.7	75	769	20.9	2050	[100]
GA + catalyst	57.8	7	–	–	84	826	20.6	1966	[102]

conditions, the efficiency reaches 40% and the energy cost for acetylene production is about 1080 kJ/mol. Further modifications, such as use of magnetic rotating arc (DuPont process) and conical shape arc, co-feeding of H_2 and higher hydrocarbons to facilitate the quenching were adopted to increase the energy efficiency. The use of H_2 as carrier gas at high concentration (up to 80%) facilitates the conversion of thermal to chemical energy and prevents diacetylene formation, which is a precursor of carbon. Consequently, higher amount of acetylene is produced (up to 76%) while carbon is minimised. To improve the energy efficiency of the process (up to 46%) a preheating step of the feeding gas with the exhaust gas is introduced. Preheated gas at 500 °C increases the acetylene yield and decreases the energy cost by 25%. Thus, the electric cost for acetylene formation decreased to 818 kJ/mol. However, thermal plasma converters are still energy demanding units due to the high thermal losses in the form of sensible heat of products (36%) and hardware (18% in cooling the plasmatron).

On the other hand, non-thermal discharges work at lower temperature, where thermal losses are lower than in thermal discharges. In principle, DBD yields the lowest efficiencies as can be seen in Table 1 ([71,85]). Nozaki et al. [63] analysed the reasons of the low efficiency using their model. At low electric field strengths, CH_3 is the main radical with a density 10 times higher than the electron density. Vibrational channel excitation has significantly lower energetic threshold (0.2–0.4 eV) as compared with the CH_4 dissociation reaction to CH_3 (9 eV); therefore, excited methane species have a density of 150 times higher than the electron density, which is typically low (10^{14} cm^{-3}) [36]. Due to the large cross-section, 36% of the input electrical energy is channelled to vibrational excitation and lost through molecular collisions [36]. In addition, heat is dissipated to dielectric material and gas heating. Eventually, the energy efficiency of C_2 production drops at about 1%. An effective way to increase the efficiency as proposed by Nozaki et al. [63] is to apply nanosecond pulsed voltage (< 10–100 ns) to suppress the undesired energy losses caused by ion current generation (resulting in gas heating). Ravasio and Cavallotti et al. [54] indicated that the voltage repetition in the same plasma volume is useful in terms of energy efficiency in pulsed discharge because at high frequencies (> 10 kHz) the memory effect facilitates the breakdown event and the energy required to initiate the microfilament decreases. However, the most effective solution is the placement of tailored catalysts inside the discharge zone; a part of thermal losses is efficiently utilized in catalytic reactions, increasing thus the efficiency. Vibrationally excited CH_4 molecules and gas temperature (expected to be higher than the catalyst bed temperature) can promote catalytic methane coupling, increasing thus the overall conversion. However, this synergic effect of plasma-assisted catalysis has not been explained yet and, experimentally, it seems contradictory. Therefore, many authors have focused their research on understanding this effect; some works confirm the improvement of performance when catalyst is present; in others, the presence of catalyst decreases the overall conversion. These works have been collected in few review papers in the last two years [151,152].

Other plasma techniques, with higher energy density have higher efficiency. Generally, the efficiency of corona and MW discharge is in the range of 4–6% at atmospheric pressure, while spark discharge, some pulsed corona discharges and GA can reach 15–20%. For such kind of macro-discharges, Ravasio and Cavallotti [54] found that high local gas temperatures are necessary to achieve high energy efficiency because the thermal decomposition of ethane and methane is activated only at high temperature. That way, the otherwise wasted thermal energy is efficiently utilized. Ravasio and Cavallotti [54] also claimed that increase in the deposited energy into the discharge, by increasing the voltage or the frequency, and decrease in the surface/volume ratio suppresses carbon formation and maximizes the thermal energy recovery from the exhaust products.

However, only two published papers reported higher efficiency and comparable or lower energy cost than the thermal processes. These are: Babarisky et al. [149], who used a MW plasma reactor at low pressure (80 mbar), and Yao and Suzuki [128] who used a pulsed discharge at atmospheric pressure. The MW discharge reached 61% efficiency and energy cost of 604 kJ/mol_{C2H2}. The authors introduced the vibrational excitation mechanism [63] to justify the results. They also reported that at high pressure, the discharge was warmer ($T_v \sim T_0$) and the higher translational temperature (T_0) promoted the conversion of acetylene into carbon while thermal losses increased. Consequently, the efficiency dropped at 6.9%. The authors concluded that it was more convenient to operate the MW plasma reactor at lower pressure, far from equilibrium ($Tv > T_0$). Under such conditions, the acetylene yield is high; carbon formation is negligible and, due to the lower gas temperature, the thermal losses are minimal. The low energy cost of C_2H_2 formation though does not take into account the energy cost of vacuum, which increases the total production cost. Further, vacuum demands more expensive and complex equipment.

Contrariwise, the pulsed discharge operates under atmospheric pressure. The efficiency (46%) and the energy cost (860 kJ/mol_{C2H2}) are comparable with the thermal process. For similar discharge configurations, Lotfalipour et al. [47] highlighted the importance of the vibrational excitation channel in CH_4 dissociation. The vibrational channel of dissociation (with an energetic barrier of 4.5 eV) dominates

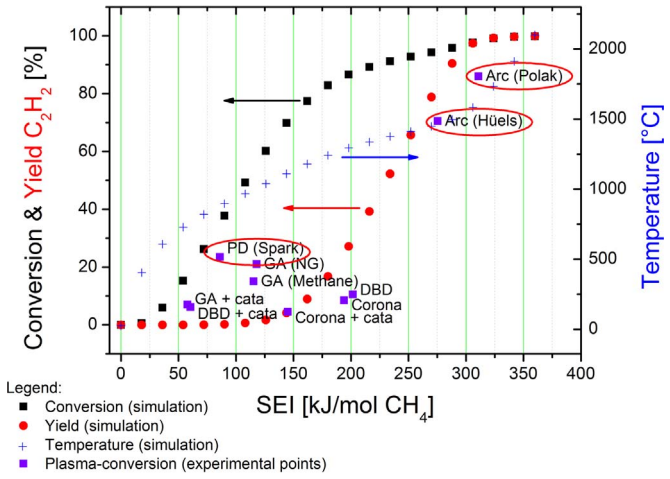

Fig. 25. Thermodynamically maximum conversion (black squares) and acetylene yield (red circles) as function of temperature and Specific Energy Input (SEI). The calculations are based on minimization of Gibbs free energy, using Aspen Plus V8.8. The experimental points are the reported ones in Table 1. (For interpretation of the references to colour in this figure legend, the reader is referred to the web version of this article.)

over the other electron impact dissociation routes, which have higher threshold energy and lower cross section, resulting in high efficiency. Although this technique seems promising, Yao and Suzuki identified that up-scaling the high frequency pulse power supply and the plasma reactor are the main bottlenecks of the technology.

The thermodynamically maximum amount of product that can be formed for a given consumed amount of energy is used as a reference to assess the plasma-driven methane efficiency. In Fig. 25, the thermodynamically maximum methane conversion and acetylene yield is presented as function of the specific energy input. The specific energy input comprises the amount of energy required for gas heating up to the specified operating temperature ($\int_{T_0}^{T} mc_p dT$) and the reaction heat of methane coupling based on the equilibrium composition at the given operating temperature.

Considering the data presented in Table 1 and the thermodynamic equilibrium of Fig. 25, DBD and corona discharges have very lower methane conversion and low acetylene yield than the thermodynamically maximum methane conversion and acetylene yield at the same specific input. GA performs better than DBD and corona but still does not reach the value imposed by the thermodynamic equilibrium for a given energy input. On the other hand, pulsed discharge, and arc show better performance, closer to the thermodynamic equilibrium.

6. Outlook

Non-oxidative methane coupling is one of the most attractive methane valorization routes leading to commodity chemicals with high commercial value especially for the polymer and chemical industry. Non-equilibrium electrical discharges, channelling the electric energy directly into molecular dissociation may be a promising alternative, for methane coupling, to conventional thermal processing, which is characterized by low equilibrium conversion and requires catalyst and high operating temperatures necessitating bulky and costly gas-fired furnaces. Major advantages of cold plasma techniques are the low operating temperature, the low thermal inertia and the fast response to fluctuating or intermittent operating conditions. However, attaining high energy efficiency is the biggest challenge towards industrialization of the plasma-driven process. High energy efficiency, may be attained through plasma performance optimization and integration of plasma and catalysis.

As regards the first aspect, on-going technological developments may permit to overcome current process limitations and open new operating windows leading to plasma performance optimization. However, these technological developments (i.e. nanosecond pulsed generators and related pulsed discharges) must be accompanied with a full comprehension of the involved physics and a clear view of the strengths and weaknesses of the latest technology use. Models and diagnostics of gas-phase plasma chemistry would considerably contribute towards this direction. Tuning and controlling the parameters that influence the plasma characteristics may also improve plasma performance. For instance, the decomposition rate increases when part of the dissipated energy is channelled into the vibrational excitation mode. Consequently, it is possible for a part of the dissipated thermal energy to be utilized in the radical chemistry, thus enhancing conversion and improving plasma performance. Different ways to channel the dissipated energy into the vibrational excitation modes might be a future research topic in gas-phase plasma chemistry.

Many efforts have been carried out to integrate plasma and catalysis in one step. It has been observed that plasma-catalyst interaction (not only for non-oxidative methane coupling) lead to a synergistic effect; conversion and selectivity, as well as energy efficiency, are affected and different products are formed, as compared to plasma alone or thermal catalytic processing. However, hybrid plasma-catalytic systems still face several challenges, some being of technical nature (i.e. coke formation and deposition resulting in catalyst deactivation and discharge suppression due to short circuits, catalyst instability and decomposition inside the discharge) and some of scientific nature (diffusion and surface chemistry enhancement by the electric field, effect of catalyst presence on the electric field pattern, nature of the reactive species that are produced by plasma and interact with the catalyst surface). Global models taking into account both gas-phase plasma chemistry and catalyst surface chemistry contributions will provide insight into the associated fundamental phenomena and plasma-catalyst interaction.

Finally, regarding technology industrialization, the first challenge is to change the perception of part of the community on plasma technologies and their applications, which are often considered energy-intensive and high-cost technologies and profitable only for specific high-tech products, such as electronics. The second challenge concerns the electric energy cost, which at present is higher compared to thermal energy that drives most chemical processes. In the future, however, the electricity cost is expected to be significantly reduced owing to the high availability of renewable energy sources and concurrent fossil fuel depletion. In this context, research on and development of electricity-based technologies is an essential step toward conversion of renewable electric energy into valuable products (power-to-chemicals concept). When these two challenges are addressed, technical issues related to technology upscaling will become less important than today.

7. Conclusions

Plasma-driven methane coupling is an alternative process for gas valorisation to added-value products. Thermal plasmas have been extensively studied and also applied at industrial scale. Lately, however, non-thermal plasmas have attracted interest and fuelled the research for deep exploration of this type of plasma in terms of different aspects; these include models development to understand the physical and chemical phenomena in the discharge, reactor design aspects, as well as experimental parametric studies to optimise the process.

Non-thermal plasmas may have moderate (cold plasmas) or higher gas temperature (warm plasmas). The gas temperature in non-thermal plasmas is crucial for the product formation and product distribution because it affects the recombination reactions and determines which reactions will be activated. Very high gas temperatures must be avoided in order to minimise the thermal losses in gas heating and increase the efficiency of the process. From this point of view, pulsed discharges are

able to control not only the chemistry during the discharge period, but also in the "switch-off" period between successive discharges, through manipulation of the pulse repetition frequency and thereby gas temperature. In particular, nanosecond pulsed voltage and high frequency are recommended for higher energy efficiency.

Achieving high product selectivity is an important challenge in plasma-driven methane coupling processes. On one hand, catalyst use inside the discharge zone could address this challenge. On the other hand, catalysts distort the electric field and the reactor performance is reduced. Consequently, the product distribution changes and CH_4 conversion may be increased or decreased. This is a common problem that is observed in many discharges (particularly in DBDs). Therefore, new catalysts, tailored-made for hybrid plasma-catalytic systems, need to be composed.

Regarding comparison of the different plasma technologies, DBD and corona discharges have poor reaction performance. GA performs better than DBD and corona. Pulsed spark and MW discharges have the highest performance, very close to thermodynamic equilibrium, which is reached in thermal arc plasma. Finally, considering the importance of energy requirement and process efficiency, some non-thermal plasmas (pulsed discharges) could compete with the industrial conventional thermal processes, represented by thermal plasma, such as the Hüels and Polak processes. Non-thermal plasma technology upscaling is a challenging aspect towards its industrialization. However, the strong motivation for efficient valorisation of methane in various forms and feedstocks in combination with the increasing utilization of renewable electricity renders plasma as a worthy technology to further investigate and develop for methane valorization.

Acknowledgement

Funding: this work has received funding from the European Union's Horizon 2020 Research and Innovation Programme through project "Adaptable Reactors for Resource and Energy Efficient Methane Valorization" (ADREM) [No. 680777].

References

[1] G. Bellussi, P. Pollesel, Industrial applications of zeolite catalysis: production and uses of light olefins, Stud. Surf. Sci. Catal. 158 (2005) 1201–1212.
[2] Y.N. Yuan, T.J. Wang, Q.X. Li, Production of low-carbon light olefins from catalytic cracking of crude bio-oil, Chin. J. Chem. Phys. 26 (2013) 237–244.
[3] S. Mokhatab, J. Mak, V. Jaleel, D. Wood, Handbook of Liquefied Natural Gas, first ed., Elsevier Inc., 2014.
[4] M. van der Hoeven, Resources to Reserves 2013: Oil Gas and Coil Technologies for the Energy Markets of the Future, (2013).
[5] D.H. Claes, The Handbook of Global Energy Policy, Wiley-Blackwell, UK, 2013.
[6] Y. Grama, The analysis of russian oil and gas reserves, Int. J. Energy Econ. Policy 2 (2012) 82–91.
[7] D. Greene, J. Hopson, J. Li, Running out of and into oil: analyzing global oil depletion and transition through 2050, Transp. Res. Rec. 1880 (2004) 1–9.
[8] M. Höök, Depletion and Decline Curve Analysis in Crude Oil Production, Uppsala, 2009.
[9] A. Jaffe, K. Medlock, R. Soligo, The Status of World Oil Reserves: Conventional and Unconventional Resources in the Future Supply Mix, Rice Univ., 2011.
[10] J. Evans, L.C. Hunt, International Handbook on the Economics of Energy, (2009), pp. 89–97.
[11] C.E. Thomas, Fuel Infrastructure Cost, In: Sustain Transp. Options 21 st Century Beyond, Springer, 2015, pp. 43–49.
[12] A. Dorsman, T. Gok, M. Baha Karan (Eds.), Perspectives on Energy Risk, Springer, 2014.
[13] C.D. Elvidge, M. Zhizhin, K. Baugh, F.C. Hsu, T. Ghosh, Methods for global survey of natural gas flaring from visible infrared imaging radiometer suite data, Energies 9 (2016) 14.
[14] J. Bingaman, Report to the Honorable Jeff Bingaman, Ranking Minority Member, Committee on Energy and Natural Resources, U.S. Senate, 2004.
[15] J. Homer, Natural Gas in Developing Countries The Intemational Bank for Reconstruction and Development, The World Bank, 1993.
[16] A. Malcolm, The Economics of the Gas Supply Industry, 1st ed., Routledge, New York, 2016.
[17] R.P. Anderson, J.R. Fincke, C.E. Taylor, Conversion of natural gas to liquids via acetylene as an intermediate, Fuel 81 (2002) 909–925.
[18] D.L. Sun, F. Wang, R.Y. Hong, C.R. Xie, Preparation of carbon black via arc discharge plasma enhanced by thermal pyrolysis, Diam. Relat. Mater. 61 (2016) 21–31.
[19] R. Utrilla, J.L. Pinilla, I. Suelves, M.J. Lázaro, R. Moliner, Catalytic decomposition of methane for the simultaneous co-production of CO_2-free hydrogen and carbon nanofibre based polymers, Fuel 90 (2011) 430–432.
[20] H. Jiang, H. Li, Y. Zhang, Tri-reforming of methane to syngas over Ni/Al_2O_3 – thermal distribution in the catalyst bed, J. Fuel Chem. Technol. 35 (2007) 72–78.
[21] E. Friederichs, T. Christoph, H. Buschmann, Ammonia, 2. production processes, Ullmann's Encycl. Ind. Chem. (2012) 295–338, http://dx.doi.org/10.1002/14356007.o02.
[22] M. Akri, T. Chafik, P. Granger, P. Ayrault, C. Batiot-Dupeyrat, Novel nickel promoted illite clay based catalyst for autothermal dry reforming of methane, Fuel 178 (2016) 139–147.
[23] M. Usman, W.M.A. Wan Daud, H.F. Abbas, Dry reforming of methane: influence of process parameters–a review, Renew. Sustain. Energy Rev. 45 (2015) 710–744.
[24] P.D.F. Vernon, M.L.H. Green, A.K. Cheetham, A.T. Ashcroft, Partial oxidation of methane to synthesis gas, and carbon dioxide as an oxidising agent for methane conversion, Catal. Today 13 (1992) 417–426.
[25] K. Supat, K. Supat, S. Chavadej, S. Chavadej, L.L. Lobban, L.L. Lobban, R.G. Mallinson, R.G. Mallinson, Combined steam reforming and partial oxidation of methane to synthesis gas under electrical discharge, Ind. Eng. Chem. (Anal. Ed.) (2003) 1654–1661.
[26] W. Jang, D. Jeong, J.-O. Shim, H. Kim, H. Roh, I.H. Son, S.J. Lee, Combined steam and carbon dioxide reforming of methane and side reactions: thermodynamic equilibrium analysis and experimental application, Appl. Energy 173 (2016) 80–91.
[27] K. Aasberg-Petersen, T.S. Christensen, C.S. Nielsen, I. Dybkjær, Recent developments in autothermal reforming and pre-reforming for synthesis gas production in GTL applications, Fuel Process. Technol. 83 (2003) 253–261.
[28] D.J. Wilhelm, D.R. Simbeck, A.D. Karp, R.L. Dickenson, Syngas production for gas-to-liquids applications: technologies, issues and outlook, Fuel Process. Technol. 71 (2001) 139–148.
[29] M. Zahedi nezhad, S. Rowshanzamir, M.H. Eikani, Autothermal reforming of methane to synthesis gas: modeling and simulation, Int. J. Hydrogen Energy. 34 (2009) 1292–1300.
[30] C. Song, W. Pan, Tri-reforming of methane: a novel concept for catalytic production of industrially useful synthesis gas with desired H_2/CO ratios, Catal. Today 2004 (2016) 463–484.
[31] J.S. Kang, D.H. Kim, S.D. Lee, S.I. Hong, D.J. Moon, Nickel-based tri-reforming catalyst for the production of synthesis gas, Appl. Catal. A Gen. 332 (2007) 153–158.
[32] J. Hong, W. Chu, M. Chen, X. Wang, T. Zhang, Preparation of novel titania supported palladium catalysts for selective hydrogenation of acetylene to ethylene, Catal. Commun. 8 (2007) 593–597.
[33] H. Jiang, H. Li, H. Xu, Y. Zhang, Preparation of $Ni/Mg_xTi_{1-x}O$ catalysts and investigation on their stability in tri-reforming of methane, Fuel Process. Technol. 88 (2007) 988–995.
[34] C. Song, W. Pan, Tri-reforming of methane: a novel concept for synthesis of industrially useful synthesis gas with desired H_2/CO ratios using CO_2 in flue gas of power plants without CO_2 separation, ACS Div. Fuel Chem. Prepr. 49 (2004) 128–131.
[35] W. Pan, J. Zheng, C. Song, Catalytic tri-reforming of methane using flue gas from fossil fuel-based power plants, Fuel Chem. Div. Prepr. 47 (2002) 262–264.
[36] T. Nozaki, K. Okazaki, Non-thermal plasma catalysis of methane: principles, energy efficiency, and applications, Catal. Today 211 (2013) 29–38.
[37] A. Holmen, O. Olsvik, O.A. Rokstad, Pyrolysis of natural gas: chemistry and process concepts, Fuel Process. Technol. 42 (1995) 249–267.
[38] M. Stöcker, Gas phase catalysis by zeolites, Microporous Mesoporous Mater. 82 (2005) 257–292.
[39] O. Deutschmann, R. Schwiedernoch, L.I. Maier, D. Chatterjee, Natural gas conversion in monolithic catalysts: interaction of chemical reactions and transport phenomena, Stud. Surf. Sci. Catal. 136 (2001) 251–258.
[40] J.R.H. Ross, A.N.J. van Keulen, M.E.S. Hegarty, K. Seshan, The catalytic conversion of natural gas to useful products, Catal. Today 30 (1996) 193–199.
[41] R.L. Van Mao, N.-T. Vu, N. Al-yassir, N. Francois, J. Monnier, The thermocatalytic cracking process for the production of light olefins and transportation fuels from gas oils, Top. Catal. 37 (2006) 107–112.
[42] S.M. Sadrameli, Thermal/catalytic cracking of hydrocarbons for the production of olefins: a state-of-the-art review I: thermal cracking review, Fuel 140 (2015) 102–115.
[43] H. Zimmermann, R. Walzl, Ethylene, Ullmann's Encycl. Ind. Chem. (2010) 465–526.
[44] D. Jones, P. Pujado, Handbook of Petroleum Processing Handbook of Petroleum Processing, Springer, 2006.
[45] H. Liang, H. Ming, S. Huei, Y. Chao, M. Been, Review of plasma catalysis on hydrocarbon reforming for hydrogen production – Interaction integration, and prospects, Appl. Catal. B Environ. 85 (2008) 1–9.
[46] M.R. Rahimpour, A. Jahanmiri, M. Mohamadzadeh Shirazi, N. Hooshmand, H. Taghvaei, Combination of non-thermal plasma and heterogeneous catalysis for methane and hexadecane co-cracking: effect of voltage and catalyst configuration, Chem. Eng. J. 219 (2013) 245–253.
[47] R. Lotfalipour, A.M. Ghorbanzadeh, A. Mahdian, Methane conversion by repetitive nanosecond pulsed plasma, J. Phys. D. Appl. Phys. 47 (2014) 365201–365216.
[48] A. Gutsol, Handbook of Combustion, Wiley-VCH, 2010.
[49] A. Indarto, N. Coowanitwong, J.W. Choi, H. Lee, H.K. Song, Kinetic modeling of plasma methane conversion in a dielectric barrier discharge, Fuel Process. Technol. 89 (2008) 214–219.

[50] C. De Bie, B. Verheyde, T. Martens, J. Van Dijk, S. Paulussen, A. Bogaerts, Fluid modeling of the conversion of methane into higher hydrocarbons in an atmospheric pressure dielectric barrier discharge, Plasma Process. Polym. 8 (2011) 1033–1058.
[51] M. Dors, H. Nowakowska, M. Jasiński, J. Mizeraczyk, Chemical kinetics of methane pyrolysis in microwave plasma at atmospheric pressure, Plasma Chem. Plasma Process 34 (2014) 313–326.
[52] A. Indarto, J. Choi, H. Lee, H.K. Song, Kinetic modeling of plasma methane conversion using gliding arc, J. Nat. Gas Chem. 14 (2005) 13–21.
[53] T. Farouk, S. Member, B. Farouk, A. Fridman, Computational studies of atmospheric-Pressure methane – hydrogen DC micro glow discharges, IEEE Trans. Plasma Sci. 38 (2010) 73–85.
[54] S. Ravasio, C. Cavallotti, Analysis of reactivity and energy efficiency of methane conversion through non thermal plasmas, Chem. Eng. Sci. 84 (2012) 580–590.
[55] Y. Yang, Direct non-oxidative methane conversion by non-thermal plasma: modeling study, Plasma Chem. Plasma Process 23 (2003) 327–346.
[56] R. Wright, Thermal Conversion of Methane to Acetylene Final Report, (2000).
[57] J.R. Fincke, R.P. Anderson, T. Hyde, B.A. Detering, R. Wright, R.L. Bewley, D.C. Haggard, W.D. Swank, Plasma thermal conversion of methane to acetylene, Plasma Chem. Plasma Process 22 (2002) 107–138.
[58] A. Fridman, Plasma Chemistry, 1st ed., Cambridge, 2008.
[59] T. Kovács, Methane conversion: a case study for simplification of plasma chemistry models by the omission of charged species, Plasma Chem. Plasma Process 30 (2010) 207–212.
[60] D.I. Slovetskii, Y.A. Mankelevich, S.D. Slovetskii, T.V. Rakhimova, Mathematical modeling of the plasma-chemical pyrolysis of methane, High Energy Chem. 36 (2002) 44–52.
[61] R. Snoeckx, M. Setareh, R. Aerts, P. Simon, A. Maghari, A. Bogaerts, Influence of N2 concentration in a CH_4/N_2 dielectric barrier discharge used for CH_4 conversion into H_2, Int. J. Hydrogen Energy 38 (2013) 16098–16120.
[62] G. Horvath, N.J. Mason, L. Polachova, M. Zahoran, L. Moravsky, S. Matejcik, Packed bed DBD discharge experiments in admixtures of N_2 and CH_4, Plasma Chem. Plasma Process 30 (2010) 565–577.
[63] T. Nozaki, A. Hattori, K. Okazaki, Partial oxidation of methane using a microscale non-equilibrium plasma reactor, Catal. Today 98 (2004) 607–616.
[64] S. Kado, K. Urasaki, Y. Sekine, K. Fujimoto, T. Nozaki, K. Okazaki, Reaction mechanism of methane activation using non-equilibrium pulsed discharge at room temperature, Fuel 82 (2003) 2291–2297.
[65] D.H. Lee, K.T. Kim, Y.H. Song, W.S. Kang, S. Jo, Mapping plasma chemistry in hydrocarbon fuel processing processes, Plasma Chem. Plasma Process 33 (2013) 249–269.
[66] R.S. Berry, The theory of penning ionization, Radiat. Res. 59 (1974) 367–375.
[67] G. Fau, N. Gascoin, J. Steelant, Hydrocarbon pyrolysis with a methane focus: a review on the catalytic effect and the coke production, J. Anal. Appl. Pyrol. 108 (2014) 1–11.
[68] U. Kogelschatz, Dielectric-barrier discharges: their history, discharge physics, and industrial applications, Plasma Chem. Plasma Process 23 (2003) 1–46.
[69] J. Lü, Z. Li, Conversion of natural gas to C2 hydrocarbons via cold plasma technology, J. Nat. Gas Chem. 19 (2010) 375–379.
[70] B. Wang, W. Yan, W. Ge, X. Duan, Methane conversion into higher hydrocarbons with dielectric barrier discharge micro-plasma reactor, J. Energy Chem. 22 (2013) 876–882.
[71] C. Xu, X. Tu, Plasma-assisted methane conversion in an atmospheric pressure dielectric barrier discharge reactor, J. Energy Chem. 22 (2013) 420–425.
[72] S.Y. Liu, D.H. Mei, Z. Shen, X. Tu, Nonoxidative conversion of methane in a dielectric barrier discharge reactor: prediction of reaction performance based on neural network model, J. Phys. Chem. C 118 (2014) 10686–10693.
[73] Y. Nishida, H.C. Chiang, T.C. Chen, T. Konishi, C.Z. Cheng, Hydrogen production from hydrocarbons using plasma: effect of discharge pulsewidth on decomposition, IEEE Trans. Plasma Sci. 43 (2015) 3500–3506.
[74] K. Konno, K. Onoe, Y. Takiguchi, T. Yamaguchi, Conversion of methane by an electric barrier-discharge plasma using an inner electrode with discharge disks set at 5 mm intervals, Chem. Eng. Res. Des. 95 (2015) 144–149.
[75] S.K. Kundu, E.M. Kennedy, V.V. Gaikwad, T.S. Molloy, B.Z. Dlugogorski, Experimental investigation of alumina and quartz as dielectrics for a cylindrical double dielectric barrier discharge reactor in argon diluted methane plasma, Chem. Eng. J. 180 (2012) 178–189.
[76] Y. Nishida, H.C. Chiang, T.C. Chen, C.Z. Cheng, Efficient production of hydrogen by DBD type plasma discharges, IEEE Trans. Plasma Sci. 42 (2014) 3765–3771.
[77] Y. Nishida, C. Cheng, K. Iwasaki, Hydrogen production from hydrocarbons with use of plasma discharges under high pressure condition, IEEE Trans. Plasma Sci. 42 (2014) 1–7.
[78] S. Jo, D. Hoon Lee, W. Seok Kang, Y.-H. Song, Methane activation using noble gases in a dielectric barrier discharge reactor, Phys. Plasmas 20 (2013) 83509.
[79] S. Jo, D.H. Lee, K.T. Kim, W.S. Kang, Y.H. Song, Methane activation using Kr and Xe in a dielectric barrier discharge reactor, Phys. Plasmas 21 (2014) 103504.
[80] S. Jo, D.H. Lee, Y.H. Song, Product analysis of methane activation using noble gases in a non-thermal plasma, Chem. Eng. Sci. 130 (2015) 101–108.
[81] B. Wang, W. Yan, W. Ge, X. Duan, Methane conversion into higher hydrocarbons with dielectric barrier discharge micro-plasma reactor, Chem. Eng. J. 22 (2013) 876–882.
[82] O. Khalifeh, A. Mosallanejad, H. Taghvaei, M.R. Rahimpour, A. Shariati, Decomposition of methane to hydrogen using nanosecond pulsed plasma reactor with different active volumes, voltages and frequencies, Appl. Energy 169 (2016) 585–596.
[83] O. Khalifeh, H. Taghvaei, A. Mosallanejad, M.R. Rahimpour, A. Shariati, Extra pure hydrogen production through methane decomposition using nanosecond pulsed plasma and Pt-Re catalyst, Chem. Eng. J. 294 (2016) 132–145.
[84] A. Górska, K. Krawczyk, S. Jodzis, K. Schmidt-Szałowski, Non-oxidative methane coupling using $Cu/ZnO/Al_2O_3$ catalyst in DBD, Fuel 90 (2011) 1946–1952.
[85] P. Kasinathan, S. Park, W.C. Choi, Y.K. Hwang, J.S. Chang, Y.K. Park, Plasma-enhanced methane direct conversion over particle-size adjusted MO_x/Al_2O_3 (M = Ti and Mg) catalysts, Plasma Chem. Plasma Process 34 (2014) 1317–1330.
[86] S. Jo, D.H. Lee, W.S. Kang, Y.H. Song, Effect of packing material on methane activation in a dielectric barrier discharge reactor, Phys. Plasmas 20 (2013) 123507.
[87] S. Jo, T. Kim, D.H. Lee, W.S. Kang, Y.H. Song, Effect of the electric conductivity of a catalyst on methane activation in a dielectric barrier discharge reactor, Plasma Chem. Plasma Process 34 (2014) 175–186.
[88] X.S. Li, A.M. Zhu, K.J. Wang, Y. Xu, Z.M. Song, Methane conversion to C_2 hydrocarbons and hydrogen in atmospheric non-thermal plasmas generated by different electric discharge techniques, Catal. Today 98 (2004) 617–624.
[89] S. Kudryashov, A. Ryabov, G. Shchyogoleva, A new approach to the non-oxidative conversion of gaseous alkanes in a barrier discharge and features of the reaction mechanism, J. Phys. D. Appl. Phys. 49 (2016) 13–26.
[90] S. Kado, Y. Sekine, T. Nozaki, K. Okazaki, Diagnosis of atmospheric pressure low temperature plasma and application to high efficient methane conversion, Catal. Today 2004 (2016) 47–55.
[91] A. Fridman, S. Nester, L.A. Kennedy, A. Saveliev, O. Mutaf-yardimci, Gliding arc gas discharge, Prog. Energy Combust. Sci. 25 (1999) 211–231.
[92] I. Rusu, J.M. Cormier, On a possible mechanism of the methane steam reforming in a gliding arc reactor, Chem. Eng. J. 91 (2003) 23–31.
[93] C.S. Kalra, Y.I. Cho, A. Gutsol, A. Fridman, T.S. Rufael, Gliding arc in tornado using a reverse vortex flow, Rev. Sci. Instrum. 76 (2005) 25110.
[94] W. Piavis, S. Turn, S.M. Ali Mousavi, Non-thermal gliding-arc plasma reforming of dodecane and hydroprocessed renewable diesel, Int. J. Hydrogen Energy 40 (2015) 13295–13305.
[95] N. Rueangjitt, T. Sreethawong, S. Chavadej, H. Sekiguchi, Plasma-catalytic reforming of methane in AC microsized gliding arc discharge: effects of input power, reactor thickness, and catalyst existence, Chem. Eng. J. 155 (2009) 874–880.
[96] D.H. Lee, K.T. Kim, M.S. Cha, Y.H. Song, Plasma-controlled chemistry in plasma reforming of methane, Int. J. Hydrogen Energy 35 (2010) 10967–10976.
[97] Z. Yuhan, Methane pyrolysis to acetylene in gliding arc plasma driven by magnetism, IEEE conference publication, 2011 International Conference on Computer Distributed Control and Intelligent Environmental Monitoring (2011) 894–896.
[98] S. Hu, B. Wang, Y. Lv, W. Yan, Conversion of methane to C_2 hydrocarbons and hydrogen using a gliding arc reactor, Plasma Sci. Technol. 15 (2013) 555–561.
[99] H. Zhang, C. Du, A. Wu, Z. Bo, J. Yan, X. Li, Rotating gliding arc assisted methane decomposition in nitrogen for hydrogen production, Int. J. Hydrogen Energy 39 (2014) 12620–12635.
[100] N. Rueangjitt, T. Sreethawong, S. Chavadej, H. Sekiguchi, Non-oxidative reforming of methane in a mini-gliding arc discharge reactor: effects of feed methane concentration, feed flow rate, electrode gap distance, residence time, and catalyst distance, Plasma Chem. Plasma Process 31 (2011) 517–534.
[101] H. Lee, H. Sekiguchi, Plasma–catalytic hybrid system using spouted bed with a gliding arc discharge: CH_4 reforming as a model reaction, J. Phys. D: Appl. Phys. 44 (2011) 274008.
[102] K. Schmidt-Szałowski, K. Krawczyk, J. Sentek, B. Ulejczyk, A. Górska, M. Młotek, Hybrid plasma-catalytic systems for converting substances of high stability, greenhouse gases and VOC, Chem. Eng. Res. Des. 89 (2011) 2643–2651.
[103] K. Schmidt-Szałowski, K. Krawczyk, M. Młotek, Catalytic effects of metals on the conversion of methane in gliding discharges, Plasma Process. Polym. 4 (2007) 728–736.
[104] M. Młotek, J. Sentek, K. Krawczyk, K. Schmidt-Szałowski, The hybrid plasma–catalytic process for non-oxidative methane coupling to ethylene and ethane, Appl. Catal. A: Gen. 366 (2009) 232–241.
[105] A. Indarto, J.W. Choi, H. Lee, H.K. Song, Effect of additive gases on methane conversion using gliding arc discharge, Energy 31 (2006) 2650–2659.
[106] D.H. Lee, Y.H. Song, K.T. Kim, J.O. Lee, Comparative study of methane activation process by different plasma sources, Plasma Chem. Plasma Process 33 (2013) 647–661.
[107] M. Goldman, A. Goldman, R.S. Sigmond, The corona discharge, its properties and specific uses, Pure Appl. Chem. 57 (1985) 1353–1362.
[108] E.M. Bazelyan, Y.P. Raizer, Spark Discharge, CRC Press, 1998.
[109] D. Pai, D. Lacoste, C. Laux, Transitions between corona, glow, and spark regimes of nanosecond repetitively pulsed discharges in air at atmospheric pressure, J. Appl. Phys. 107 (2010) 093303.
[110] I. Aleknaviciute, T.G. Karayiannis, M.W. Collins, C. Xanthos, Methane decomposition under a corona discharge to generate CO_x-free hydrogen, Energy 59 (2013) 432–439.
[111] S. Kado, K. Urasaki, Y. Sekine, K. Fujimoto, Direct conversion of methane to acetylene or syngas at room temperature using non-equilibrium pulsed discharge, Fuel 82 (2003) 1377–1385.
[112] A. Beloqui Redondo, E. Troussard, J.A. Van Bokhoven, Non-oxidative methane conversion assisted by corona discharge, Fuel Process. Technol. 104 (2012) 265–270.
[113] G. Horvath, M. Zahoran, N.J. Mason, S. Matejcik, Methane decomposition leading to deposit formation in a DC positive CH_4-N_2 corona discharge, Plasma Chem. Plasma Process 31 (2011) 327–335.
[114] M.A. Malik, D. Hughes, A. Malik, S. Xiao, K.H. Schoenbach, Study of the

production of hydrogen and light hydrocarbons by spark discharges in diesel kerosene, gasoline, and methane, Plasma Chem. Plasma Process 33 (2013) 271–279.
[115] M.M. Moshrefi, F. Rashidi, H.R. Bozorgzadeh, S.M. Zekordi, Methane conversion to hydrogen and carbon black by DC-spark discharge, Plasma Chem. Plasma Process 32 (2012) 1157–1168.
[116] M.M. Moshrefi, F. Rashidi, Hydrogen production from methane by DC spark discharge: effect of current and voltage, J. Nat. Gas Sci. Eng. 16 (2014) 85–89.
[117] B. Wang, H.M. Guan, Highly efficient conversion of methane to olefins via a recycle-Plasma-Catalyst reactor, Catal. Lett. 146 (2016) 2193–2199.
[118] K. Wang, X. Li, A. Zhu, A green process for high-concentration ethylene and hydrogen production from methane in a plasma-followed-by-catalyst reactor, Plasma Sci. Technol. 13 (2011) 77–81.
[119] S. Kado, Y. Sekine, K. Urasaki, K. Okazaki, T. Nozaki, High performance methane conversion into valuable products with spark discharge at room temperature, Stud. Surf. Sci. Catal. 147 (2004) 577–582.
[120] Y. Yang, Direct non-oxidative methane conversion by non-Thermal plasma: experimental study, Plasma Chem. Plasma Process 23 (2003) 283–296.
[121] A. Zhu, W. Gong, X. Zhang, B. Zhang, Coupling of methane under pulse corona plasma (I) — In the absence of oxygen, Sci. China Ser. B 43 (2000) 208–214.
[122] A. Zhu, X. Zhang, X. Li, W. Gong, Beyond-thermal-equilibrium conversion of methane to acetylene and hydrogen under pulsed corona discharge, Sci. China Ser. B. 45 (2002) 426–434.
[123] B. Dai, X. Zhang, L. Zhang, W. Gong, R. He, W. Lu, X. Deng, Study on the hydrogenation coupling of methane, Sci. China Ser. B Chem. 44 (2001) 191–195.
[124] A. Zhu, X. Zhang, W. Gong, G.-H. Zheng, Dehydrogenative coupling of methane underpulse corona plasma over a MnOx/γ-Al2O3 catalyst, J. Nat. Gas Chem. 8 (1999) 47–52.
[125] K. Wang, X. Li, H. Wang, C. Shi, Y. Xu, A. Zhu, Oxygen-free conversion of methane to ethylene in a plasma-followed-by-catalyst (PFC) reactor, Plasma Chem. Plasma Process 10 (2008) 600–604.
[126] X. Li, C. Lin, C. Shi, Y. Xu, Y. Wang, A. Zhu, Stable kilohertz spark discharges for high-efficiency conversion of methane to hydrogen and acetylene, J. Phys. D. Appl. Phys. 41 (2008) 175203.
[127] G. Zhao, S. John, J. Zhang, L. Wang, S. Muknahallipatna, J.C. Hamann, J.F. Ackerman, M.D. Argyle, O.A. Plumb, Methane conversion in pulsed corona discharge reactors, Chem. Eng. J. 125 (2006) 67–79.
[128] S.L. Yao, E. Suzuki, N. Meng, A. Nakayama, A high-efficiency reactor for the pulsed plasma conversion of methane, Plasma Chem. Plasma Process 22 (2002) 225–237.
[129] A.M. Ghorbanzadeh, N.S. Matin, Methane conversion to hydrogen and higher hydrocarbons by double pulsed glow discharge, Plasma Chem. Plasma Process 25 (2005) 19–29.
[130] Y.A. Lebedev, Microwave discharges: generation and diagnostics, J. Phys. Conf. Ser. 257 (2010) 12016.
[131] C. Shen, Y. Sun, D. Sun, H. Yang, A study on methane coupling to acetylene under the microwave plasma, Sci. China Chem. 53 (2010) 231–237.
[132] C. Shen, D. Sun, H. Yang, Methane coupling in microwave plasma under atmospheric pressure, J. Nat. Gas Chem. 20 (2011) 449–456.
[133] J. Mizeraczyk, M. Jasiński, H. Nowakowska, Studies of atmospheric-pressure microwave plasmas used for gas processing, Nukleonika 57 (2012) 241–247.
[134] M. Jasínski, M. Dors, H. Nowakowska, G.V. Nichipor, J. Mizeraczyk, Production of hydrogen via conversion of hydrocarbons using a microwave plasma, J. Phys. D: Appl. Phys. 44 (2011) 194002–194007.
[135] M. Jasiński, D. Czylkowski, B. Hrycak, M. Dors, J. Mizeraczyk, Atmospheric pressure microwave plasma source for hydrogen production, Int. J. Hydrogen Energy 38 (2013) 11473–11483.
[136] J.J. Zhang, Y. Yang, Q. Liu, K. Tan, Non-oxidative coupling of methane to C_2 hydrocarbons under above-atmospheric pressure using pulsed, Energy Fuels 16 (2002) 687–693.
[137] C.H. Tsai, K.T. Chen, Production of hydrogen and nano carbon powders from direct plasmalysis of methane, Int. J. Hydrogen Energy 34 (2009) 833–838.
[138] M. Heintze, M. Magureanu, Methane conversion into acetylene in a microwave plasma: optimization of the operating parameters, J. Appl. Phys. 2276 (2008) 2–10.
[139] M. Heintze, M. Magureanu, M. Kettlitz, Mechanism of C_2 hydrocarbon formation from methane in a pulsed microwave plasma, J. Appl. Phys. 92 (2002) 7022–7031.
[140] M. Heintze, M. Magureanu, Methane conversion into aromatics in a direct plasma-catalytic process, J. Catal. 206 (2002) 91–97.
[141] W. Cho, Y.C. Kim, S.S. Kim, Conversion of natural gas to C_2 product, hydrogen and carbon black using a catalytic plasma reaction, J. Ind. Eng. Chem. 16 (2010) 20–26.
[142] R.S. Besser, P.J. Lindner, Microplasma reforming of hydrocarbons for fuel cell power, J. Power Sources 196 (2011) 9008–9012.
[143] D.W. Wang, T.C. Ma, Y.T. Zhang, Study on natural gas converted to C2 hydrocarbons in plasma state, Adv. Mater. Res. 383–390 (383) (2011) 2894—.
[144] Z. Ghorbani, P. Parvin, A. Reyhani, S.Z. Mortazavi, A. Moosakhani, M. Maleki, S. Kiani, Methane decomposition using metal-assisted nanosecond laser-induced plasma at atmospheric pressure, J. Phys. Chem. C. 118 (2014) 29822–29835.
[145] M. Ding, T. Hayakawa, C. Zeng, Y. Jin, Q. Zhang, T. Wang, L. Ma, Y. Yoneyama, N. Tsubaki, Direct conversion of liquid natural gas (LNG) to syngas and ethylene using non-equilibrium pulsed discharge, Appl. Energy 104 (2013) 777–782.
[146] M. Yu, L.Y. Zhai, Q. Zhou, C.P. Li, X.L. Zhang, Ionic liquids as novel catalysts for methane conversion under a DC discharge plasma, Appl. Catal. A: Gen. 419–420 (2012) 53–57.
[147] X. Zhang, L. Di, Q. Zhou, Methane conversion under cold plasma over Pd-containing ionic liquids immobilized on γ-Al_2O_3, J. Energy Chem. 22 (2013) 446–450.
[148] L.S. Polak, Low-temperature plasma in petroleum chemistry, Pet. Chem. U.S.S.R. 7 (1967) 136–152.
[149] A.I. Babaritsky, S.A. Diomkin, V.K. Givotov, V.G. Makarenko, S.A. Nester, V.D. Rusanov, A. Fridman, Non-equilibrium approach to methane conversion into acetylene in microwave discharge, Kurchatov Inst. Atom. Energy 5350/12 (1991).
[150] A. Czernichowski, P. Czernichowski, Pyrolysis of natural gas in the gliding electric discharges, 10th Canadian Hydrogen Conference (2000).
[151] E.C. Neyts, K.K. Ostrikov, M.K. Sunkara, A. Bogaerts, Plasma catalysis: synergistic effects at the nanoscale, Chem. Rev. 115 (2015) 13408–13446.
[152] H.H. Kim, Y. Teramoto, A. Ogata, H. Takagi, T. Nanba, Plasma catalysis for environmental treatment and energy applications, Plasma Chem. Plasma Process 36 (2016) 45–72.